600879

ARL 64-55
APRIL 1964

Aerospace Research Laboratories

74 - p - $2.00

LINEAR STRAIN THEORY AND THE SMITH METHOD FOR PREDICTING FATIGUE LIFE OF STRUCTURES FOR SPECTRUM TYPE LOADING

CLARENCE R. SMITH
GENERAL DYNAMICS/CONVAIR
SAN DIEGO, CALIFORNIA

OFFICE OF AEROSPACE RESEARCH

United States Air Force

DDC-SD
147650

NOTICES

500 - May 1964 - 162-26-781

ARL 64-55

LINEAR STRAIN THEORY AND THE SMITH METHOD FOR PREDICTING FATIGUE LIFE OF STRUCTURES FOR SPECTRUM TYPE LOADING

CLARENCE R. SMITH

GENERAL DYNAMICS/CONVAIR
SAN DIEGO, CALIFORNIA

APRIL 1964

Contract AF 33(616)-8228
Project 7063
Task 7063-02

AEROSPACE RESEARCH LABORATORIES
OFFICE OF AEROSPACE RESEARCH
UNITED STATES AIR FORCE
WRIGHT-PATTERSON AIR FORCE BASE, OHIO

FOREWORD

This report was prepared by the Fatigue Laboratory - Engineering Department General Dynamics/Convair of San Diego, California, under United States Air Force Contract No. AF33(616)-8228. This contract was initiated by the Aeronautical Research Laboratories, Office of Aerospace Sciences, under Project-Task 7063-02 "Research in the Mechanics of Structures." It was administered under the direction of Mr. Charles A. Davies, Project Scientist, Thermo-mechanics Research Branch.

This report covers work performed in the period of May 1961 through December 1963.

Convair personnel who made major contributions to this program were: C.R. Smith, design specialist; G.D. Lindeneau, research test engineer; and R.B. Alden and E.J. Wehrhan, technicians. Thanks are also due Mr. G.G. Green, chief of structures, for guidance during the program. The data were recorded in Convair log books 4133 and 4143. This report is identified internally as GDC-63-113, December 1963 (unclassified).

ABSTRACT

Theoretical and test data are presented for two methods of predicting fatigue life. The first method requires preknowledge of stress concentration and nominal stress; the second requires preknowledge of neither. Both employ smooth specimen S-N curves and consider effects of stresses at a concentration.

The first method, the Linear Strain Theory, assumes that strain at the concentration is proportional to load within practical limits. Stress at the concentration, including residual stress, can therefore be obtained from conventional stress-strain curves, and these stresses are then used in conjunction with S-N curves to evaluate fatigue life.

The second method, the Smith Method, requires the life of a given structure in terms of a loading that is sufficiently high to ensure local yielding, which corresponds to a lifetime of less than 10,000 cycles for 7075-T6 and 40,000 cycles for 2024-T3. The unique feature of the latter method is that it does not require knowledge of either nominal stresses or stress at the concentration, stress at the concentration being obtained directly from smooth specimen test data for the material from which the structure is fabricated. The stresses thus obtained are proportioned directly with the known loading, taking into account residual stresses and the order in which loads are applied.

TABLE OF CONTENTS

SECTION		PAGE
I	INTRODUCTION	1
	DEFINING FATIGUE LIFE	1
	CRACK PROPAGATION	1
	CRACK INITIATION	1
	LINEAR STRAIN THEORY	2
	SMITH METHOD	3
II	LINEAR STRAIN THEORY	4
	STRAIN AS A FUNCTION OF STRESS AT A CONCENTRATION	4
	NUMERICAL EXAMPLE	7
	MAXIMUM RETAINABLE RESIDUAL STRESS	7
	THE S-N CURVE	7
III	THE SMITH METHOD	14
	STRESS AT A CONCENTRATION	14
	STEPS IN THE SMITH METHOD	17
IV	TEST PROGRAM	18
	FIXTURES	20
	TEST RESULTS	23
V	CORRELATION BETWEEN TEST AND THEORETICAL RESULTS	31
VI	CONCLUSIONS	33
VII	APPENDIX	35
VIII	REFERENCES	64

LIST OF TABLES

TABLE		PAGE
I	Mechanical properties of materials	35
II	Constant amplitude fatigue data for smooth axially loaded specimens of 0.1-inch thick 7075-T6 aluminum alloy	36
III	Constant amplitude fatigue data for smooth axially loaded specimens of 0.1-inch thick 2024-T3 aluminum alloy	42
IV	Constant amplitude fatigue data for smooth axially loaded specimens of 0.1-inch thick 2024-T81 aluminum alloy	44
V	Constant amplitude fatigue data for lug specimens ($K_t = 3.6$) of 7075-T6 aluminum alloy	46
VI	Constant amplitude fatigue data for lug specimens of 2024-T3 aluminum alloy	50
VII	Constant amplitude fatigue data for center hole notched specimens of 2024-T3, 2024-T81, and 7075-T6 aluminum alloy	56
VIII	Effect of bolt interference on fatigue life of 7075-T6 aluminum alloy lugs	57
IX	Effect of prestress on fatigue life of 7075-T6 aluminum alloy lugs	59
X	Results of spectrum tests on lug specimens of 7075-T6 aluminum alloy	60
XI	Results of spectrum tests on lug specimens of 2024-T3 aluminum alloy	61
XII	Results of spectrum tests on center hole specimens	62
XIII	Results of spectrum tests on smooth axially loaded specimens of 7075-T6 aluminum alloy	63

LIST OF ILLUSTRATIONS

FIGURE NO.		PAGE NO.
1	Stress-Strain Curve for 7075-T6 Aluminum Alloy Sheet	5
2	Stress as a Function of Strain at Point of Stress Concentration--Residual Compressive Stress in Unloaded Position	6
3	Stress as a Function of Strain at Point of Stress Concentration--Large Deformations	6
4	S-N Curves for 7075-T6 Aluminum Alloy Sheet	8
5	Stress Cycles at the Concentration for Specimens Having $K_t = 4$	10
6	Stress Cycles at the Concentration for Specimens Having $K_t = 4$--After High Loading	10
7	Spring Analogies of Stress Cycles at Edge of Open Hole, and at Edge of Rivet-Filled Hole	11
8	S-N Curves for Riveted Lap Joints with Various Preloads (Data from Reference 17)	13
9	S-N Curves for 7075-T6 with Maximum Stress Cutoff	16
10	Lug Specimen	19
11	Smooth Specimen	19
12	Fixture for Lug Specimens	21
13	Lateral Support Fixture for Smooth Specimens	21
14	Schedules for Spectrum Loading	22
15	S-N Curves for 2024-T3 Aluminum Alloy Sheet	24
16	S-N Curves for 2024-T81 Aluminum Alloy Sheet	25
17	Comparison of Spectrum Test Results with Predicted Lives of Notched Specimens by the Linear Strain and Smith Methods	26

LIST OF ILLUSTRATIONS, Continued

FIGURE NO.		PAGE NO.
18	Comparison of Spectrum Tests Results with Predicted Lives of Smooth Specimens	27
19	S-N Curves for 7075-T6 Lugs--Stress Due to 0.003-inch Interference is Indicated by Intersection of Curves	28
20	S-N Curves for 2024-T3 Lugs--Stress Due to 0.003-inch Interference Indicated by Intersection of Curves	29
21	Comparison of Spectrum Test Results of Full Scale Structures with Predictions by Smith Method	30

SECTION I

INTRODUCTION

DEFINING FATIGUE LIFE

The purpose of any theory for predicting fatigue life is to know how long a structure will last in service. This necessitates a definition of exactly what is meant by fatigue life. Is it from the time when the first load is applied until a crack is formed, or until the structure fails to carry a specified load? Or again, is it the interval from appearance of first crack to catastrophic failure? Some schools of thought describe fatigue as a progression of incipient cracks from the very first cycle, where the incipient crack is defined as a cloister of dislocations at a grain boundary. This would infer that the time consumed in initiating a crack is negligible.

From an economic standpoint, the fatigue failure might be considered to occur when a crack has to be repaired. In keeping with generally accepted safety patterns, no airplane operator will continue to fly an airplane with known cracks in a primary structure, even though test data have shown the structure to be safe for specified time limits. The operator, however, has to accept the fact that a crack could initiate between inspections, and he needs assurance that the airplane will be safe until the next inspection.

CRACK PROPAGATION

Life prediction to catastrophic crack length or to dangerous crack length are both couched in terms of crack propagation based on structural experience from initiation of the first crack until failure of the structure.

Work on crack propagation has come into its own during the last decade with major contributions from Irwin[1], Hardrath and McEvily[2], Paris[3], and Valluri[4]. Earlier work by Orowan[5] and Griffith[6] form needed background for most of the work concerning initiation and growth of cracks. Valluri has taken the stress in the plastic enclave area ahead of the crack to derive expressions for fatigue life, including the manner of loading, which was confirmed by comparing with smooth specimen data of 2024-T3 aluminum alloy.

CRACK INITIATION

In Terms of Load

Most theories on fatigue based on crack initiation amount to a curve-fitting of some sort. Miner[7] assumes that fatigue damage is accumulated at a linear rate, implying that if a structure would fail after N_1 cycles for cyclic loading of P_1, after N_2 cycles for P_2, and after N_n

cycles for loading of P_n — then that structure could sustain a spectrum of loads up to the time when

$$\sum n_1/N_1 + n_2/N_2 + \ldots n_n/N_n = 1$$

where n_1, n_2, and n_3 are the number of cycles applied at loads P_1, P_2, and P_3, respectively.

While the Miner or Palmgren[8] method is the most commonly accepted, mainly because of its simplicity, it can be very unconservative in some instances, and ultraconservative in others. Its biggest misfortune lies in not considering the effect that the order of loading has upon subsequent fatigue life.

In Terms of Stress

Freudenthal[9] has developed empirical relationships taking into account what he calls "Stress Interaction," which satisfy the cumulative damage type of tests for rotary beam specimens. Unfortunately, Freudenthal's work was based on rotary beam tests, which can be used to load in reverse bending only. While this may not have been too serious a handicap where no plastic deformation is involved, local yielding, as in the case of notched specimens, will always leave a residual compressive stress on one side with a residual tensile stress at the opposite side. The residual tensile stress will be directly additive with subsequent loading at lower stress levels.

This would wrongly imply that a structure would always suffer a loss in fatigue life as a result of high preloading. The opposite is usually true in axially loaded structures because the high load enhances fatigue strength by introducing a residual compressive stress at the stress concentration. In some cases, where loosening of interference bolts or rivets accompanies high loading, it is true that a loss in fatigue strength can be expected.[10] Dolan[11] has taken effects of loading order into account by correcting the slope of the S-N curve, using an exponential factor that is derived experimentally.

Of all the theories for fatigue life prediction, the Miner appeals most to the intuition because a physical model of the process can be easily visualized. While multiplying the Miner results by some factor to agree with experimental data might be appealing also, the physical concept of such a factor is lacking in most cases.

LINEAR STRAIN THEORY

This study endeavors to retain a physical concept by considering the correction as related to the residual stress left by high loading. Such an approach was first proposed by the author[12] in 1944, and the Linear Strain Theory that evolved was given experimental support by two-step loading in small specimens of 24 ST aluminum alloy. There, the assumption was made that the strain at a concentration was proportional to nominal load, and that actual stress at the concentration could be determined from a stress-strain curve for the material. The difference between the point on the stress-strain curve and a theoretical value (found by multiplying the nominal stress times the theoretical stress concentration factor) was considered a function of the residual stress in the unloaded position. This difference had to be further multiplied by an assumed ratio between plastically- and elastically-deformed material, a value of 4/7 being used to agree with observed test data.

Independent research by Gunn[13] reported a similar approach to fatigue life prediction, and Grumman Aircraft Engineering[14] now uses a Neuber notch (K_n) instead of K_t with essentially the same method. The Grumman method assumes no increase in stress above the yield strength.

All three of the linear strain methods consider failure as the initiation of a visible crack. Requirements of all three are S-N curves for axially loaded smooth specimens and the theoretical stress concentration. The Neuber notch is directly related to the theoretical value.

Unfortunately, the means are not always at hand for analyzing a structure in terms of theoretical stress concentration. For such an analysis, real fatigue data are needed — either in the form of (1) S-N data based on constant load amplitude tests or (2) S-N data based on spectrum type tests simulating anticipated service loads of the structure. The hard fact is that very little is known about the actual load spectra for a given structure during the design stage, so spectrum type tests are not likely to represent the actual loading that will be found at a later date only after in-service usage. As for the constant amplitude loading, a way must be found to relate this to the actual loads that will be experienced in service.

SMITH METHOD

Toward achieving this end, the Smith Method has been introduced.[15] Unlike the Miner method, which directly prorates the damage according to S-N characteristics of the structure, the Smith method ascertains the stress at the concentration from constant amplitude data. This is not the fatigue strength reduction factor[16], generally referred to as K_f. Rather, the stress at the point of failure is obtained directly from fatigue data. Accordingly, there is no need for knowing the nominal stress, so long as the loads producing failure are known. Stress that produces failure for a known loading is prorated directly for other loading, and the resulting ratio can be used with S-N curves for smooth axially loaded specimens to predict lives for the new load. As in the Linear Strain method, residual stresses introduced by high loading are considered in estimating fatigue at subsequent lower level loading.

The purpose of this investigation is to obtain a simple method of predicting fatigue life for program loading. By developing both the Linear Strain and the Smith Methods, it is hoped that the one will be suitable where good theoretical values for stress concentration are known and the other will be suitable where neither nominal stress nor stress concentration can be established analytically.

SECTION II

LINEAR STRAIN THEORY

STRAIN AS A FUNCTION OF STRESS AT A CONCENTRATION

A conventional approach to predicting fatigue life is through the use of geometrical or theoretical stress concentration factors in conjunction with assumed operating stresses and S-N curves for the material. Unfortunately, most structures occasionally are subjected to loads that exceed the elastic limit for the material, and the stress concentration per se does not define the stress under these loading conditions. Furthermore, after a single application of such a high load, the behavior of the structure is no longer the same as prior to high loading, even though stresses at the concentration may behave in an elastic manner.

In order to avoid having to assume an "effective" stress concentration for plastic behavior, the Linear Strain Theory approaches the problem by assuming that the strain at the concentration is proportional to the strain away from the concentration, even though inelastic deformation takes place locally. Since strain is a geometrical dimension, the state of stress should not be directly applicable. Knowing the stress-strain relation for the material, however, it is possible to obtain stress directly from a stress-strain curve for the material. Stress values obtained in this manner can then be used directly with smooth specimen S-N curves for relating fatigue life.

Mathematical and experimental evaluations of stresses at a concentration[17] most commonly agree upon a factor of 3 for a hole in an infinitely wide sheet in tension. For example, a nominal stress of 25,000 psi would cause the actual stress at the concentration to be 3 times 25,000, or 75,000 psi. In the case of 7075-T6 aluminum alloy, higher loading would cause yielding at the concentration — in fact, some permanent deformation can be expected even at 75,000 psi for material with the characteristic stress-strain curve shown in Figure 1. Obviously, stress at the concentration could not appreciably exceed the yield value without also yielding material in adjacent areas. In the case of 7075-T6 aluminum alloy and other alloys having stress-strain curves which are fairly flat above the yield point, the local strain could exceed the nominal yield value by substantial amounts without appreciably increasing the stress at the concentration. This would imply that strain could be substituted for stress in conjunction with stress concentration factors for obtaining stress where local inelastic deformation occurs. Whether the strain in the plastically deformed area is proportional to the nominal strain is problematical, however, larger errors in strains estimated in this manner could be tolerated without appreciably affecting the corresponding stress values.

A stress-strain curve for 7075-T6 is presented in Figure 2. Considering only the stress at a point of concentration, the stress-strain relationship can be assumed to follow the same pattern as that described by the curve for the parent material — at least while load is increasing. On removal of load, however, a straight-line path parallel to the original modulus will be followed until the original zero position is reached. Below this point, the plastically deformed material at the concentration (being very small by comparison with the adjacent

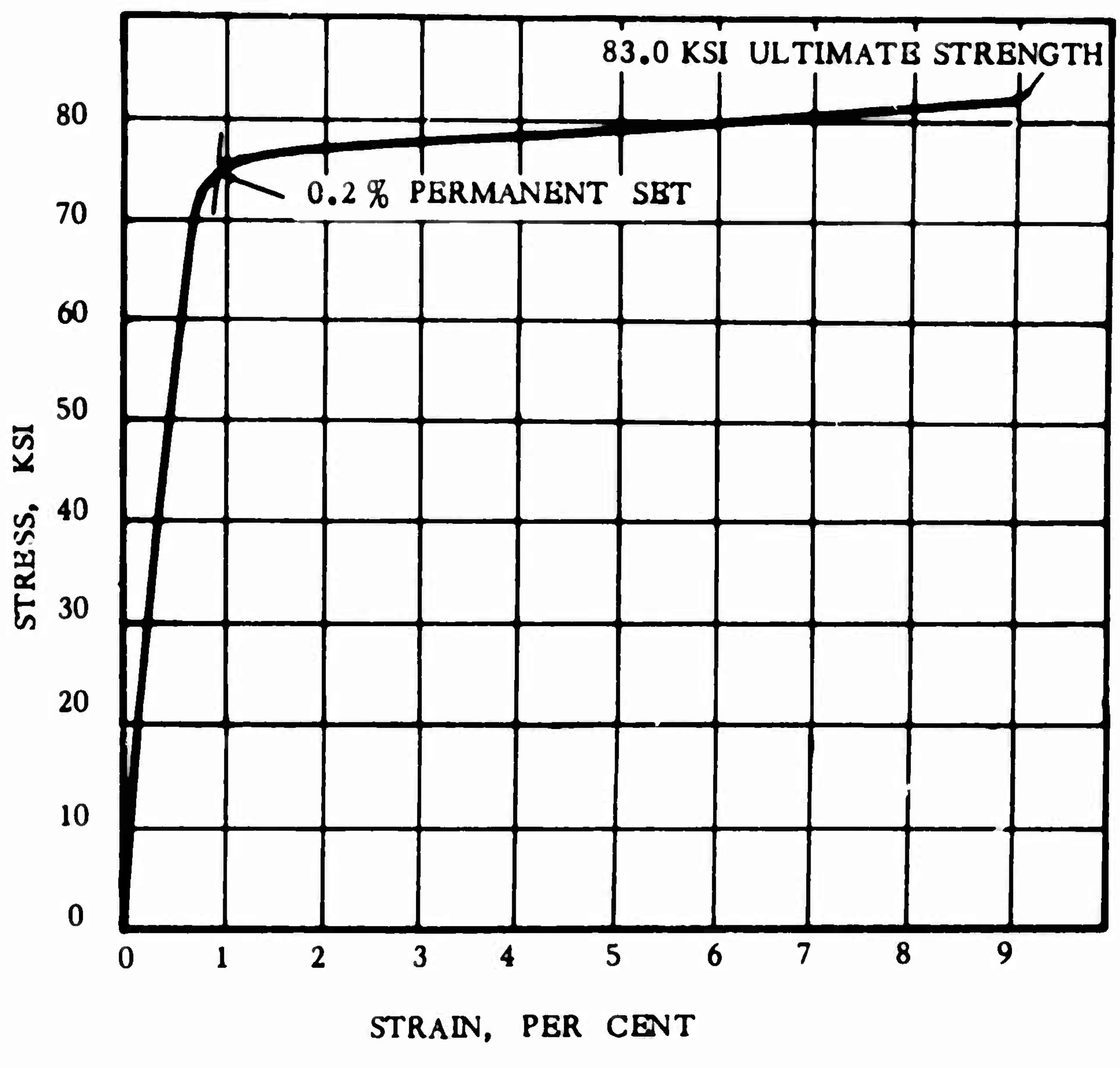

Figure 1. Stress-Strain Curve for 7075-T6 Aluminum Alloy Sheet

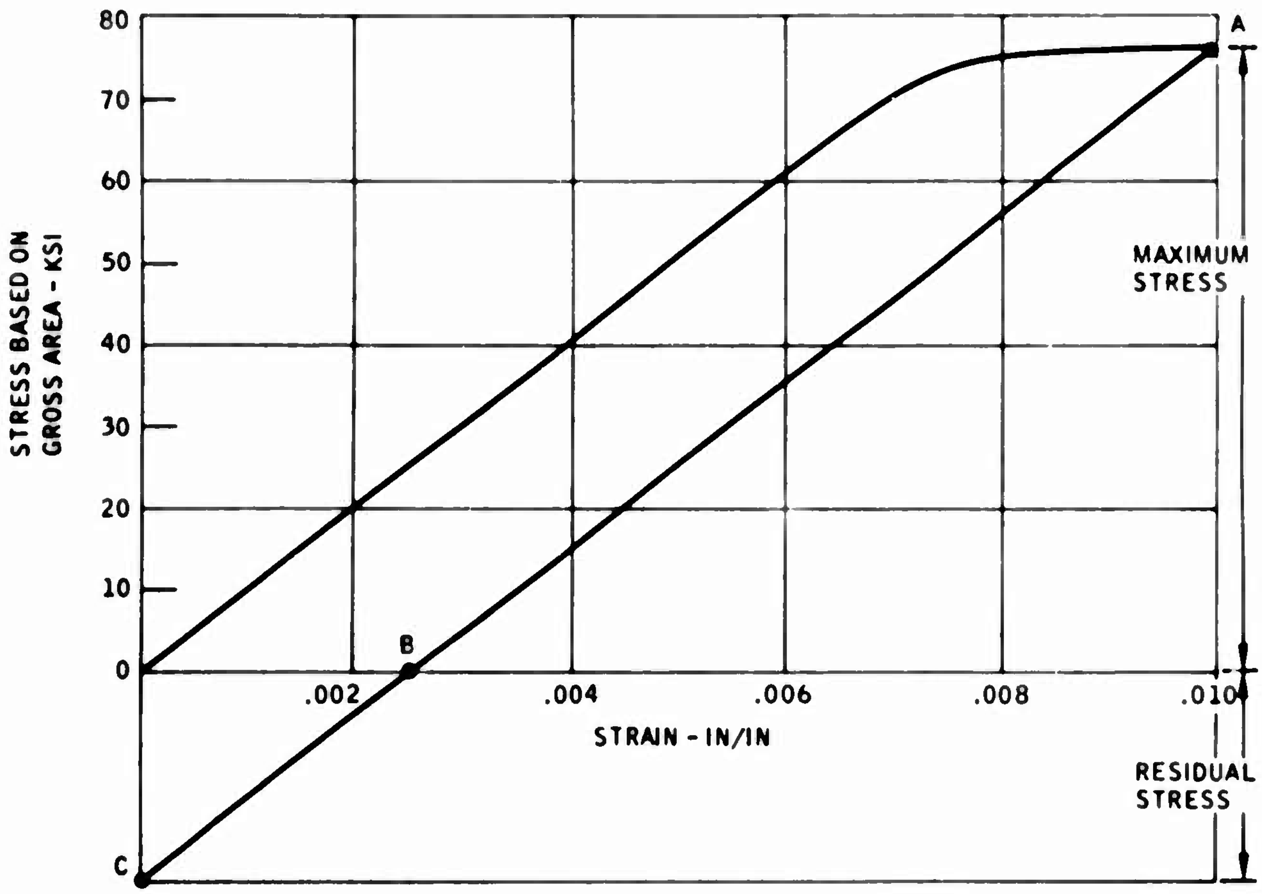

Figure 2. Stress as a Function of Strain at Point of Stress Concentration-- Residual Compressive Stress in Unloaded Position

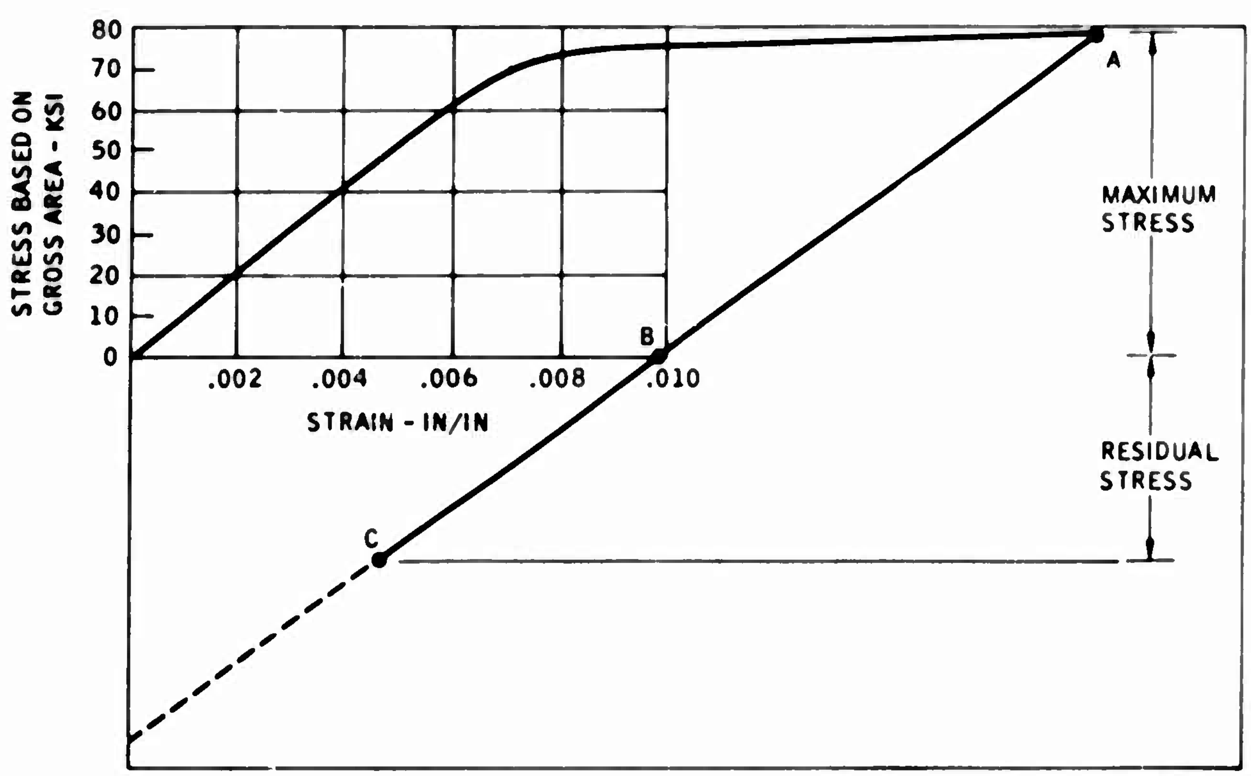

Figure 3. Stress as a Function of Strain at Point of Stress Concentration-- Large Deformations

unyielded material to which it is still attached) has to go into compression because the unyielded material has not reached the point of zero stress. The amount of compression imposed on the plastically deformed material will be determined by the proportion of the area of material plastically deformed to the area of material still in the elastic range.

NUMERICAL EXAMPLE

As a specific example, let us assume that the maximum strain at the point of concentration was 0.009 in./in. Assuming a modulus of elasticity E of 10,000,000 psi, this would conform with a stress range of 90,000 psi if the material behaved elastically. Being beyond the proportional limit for the material, it is obvious that this would not hold for the original load cycle; however, on unloading, it would be easy to visualize a stress range of this magnitude being acquired if part of the stress could be in compression. Thus, consider the case where the maximum stress at 0.009 in./in. strain is 75,000 psi and the area of the elastically deformed material is very large as compared with inelastic material. After removal of a single load causing 0.009 in./in. strain at the concentration, the compressive stress remaining would be 90,000 - 75,000, or 15,000 psi.

MAXIMUM RETAINABLE RESIDUAL STRESS

Similarly, increased values of tensile deformation would cause greater amounts of permanent set with correspondingly greater values of residual stress. However, it would be inconceivable that a residual stress greater than the compressive yield for the material could be introduced, no matter how high the preceding tensile load. Even if it were possible to introduce a greater amount, given time, the residual stress would relax to a value below the compressive yield. Actual retainable values are not known; however, experience in the shot-peening industry indicates that up to two-thirds of the compressive yield strength can be retained indefinitely at ambient temperature. This would correspond to point C in Figure 3.

THE S-N CURVE

A conventional method of presenting fatigue data is the curve showing stress as a function of the total number of cycles. Figure 4 shows a family of curves for smooth axially loaded specimens of 7075-T6 aluminum alloy. Each curve in the family corresponds to a given type of loading. For example, where the stress ratio R is defined as the minimum stress divided by the maximum stress, the curve for R = 0 would represent a repeated loading from 0 to maximum stress. Similarly, completely reversed loading is described by the curve for R = -1. Other values are presented in the curves for R = 0.5, -0.5, -2, and -4.

Where the stress range is defined as the difference between the maximum and minimum stresses, it can be seen that, for the same stress range there will be a longer life with reversed loading than with repeated loading. For example, where the maximum stress for R = 0 is 60,000 psi, the fatigue life is 28,000 cycles. The maximum stress for R = -1, having a 60,000-psi range, would be 30,000 psi. Here, the life would be 54,000 cycles.

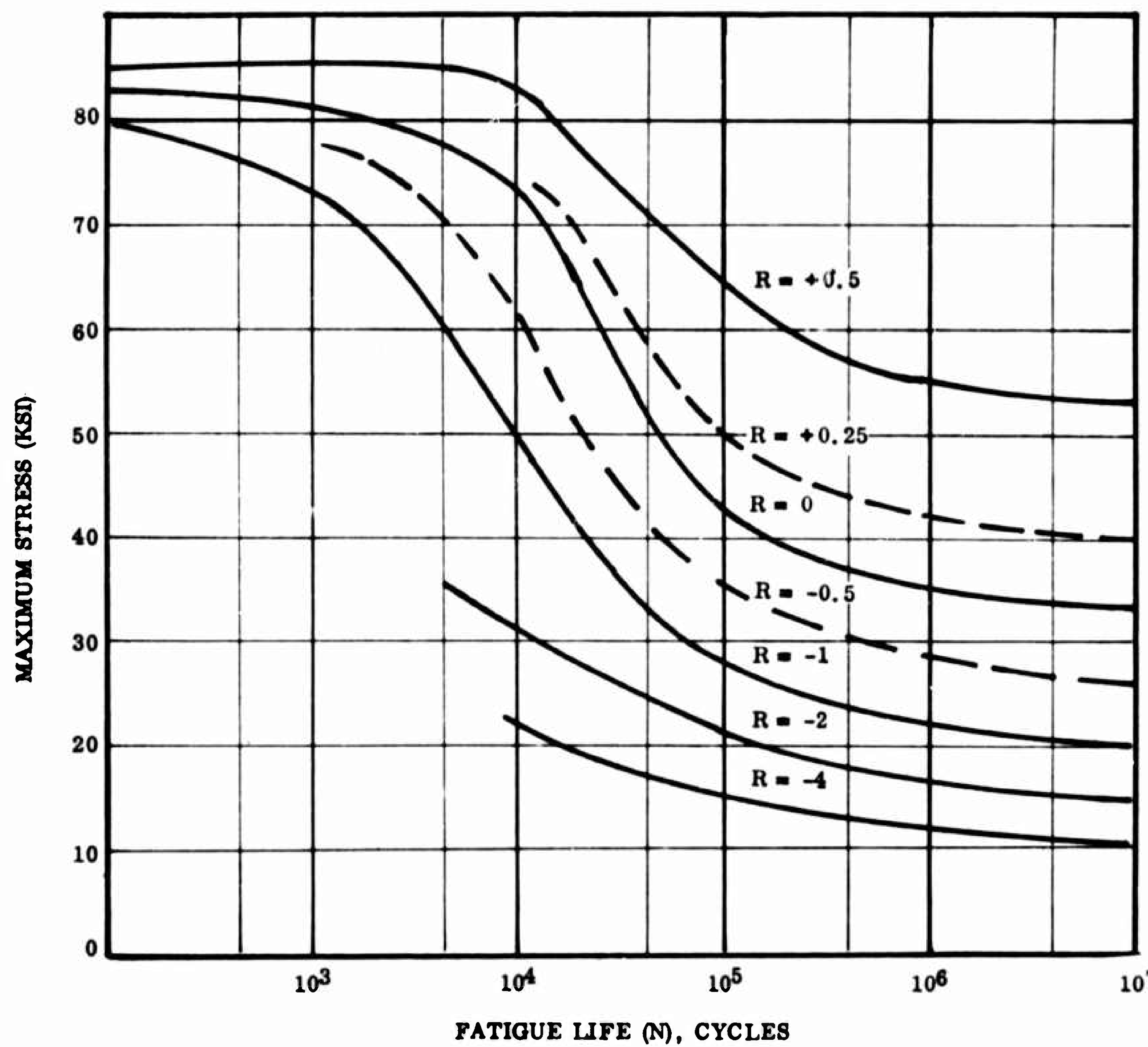

Figure 4. S-N Curves for 7075-T6 Aluminum Alloy Sheet

Since the fatigue failure of a structure will always occur at a stress concentration, it can be easily seen that high loads in a spectrum may introduce residual stresses that would influence the life for subsequent lower loading. A typical example of how fatigue life may be changed is given in Figures 5 and 6.

Figure 5A shows a typical sine wave for nominal stress cycles from 0 to 10,000 psi. For a structure having a stress concentration factor K_t of 4, a cyclic pattern from 0 to 40,000 psi could be anticipated for the same loading with a corresponding lifetime of 150,000 cycles as given in S-N curve for R = 0 (Figure 4). Nominal stress cycling of 15,000 psi would result in maximum stresses of 60,000 psi for a life of 28,000 cycles as shown schematically in Figure 5B. Figure 5C shows the case of 25,000 psi nominal stress loading. Here, whereas nominal cycling is from zero to maximum loading, the corresponding stress cycling at the concentration ranges from a negative value to about the yield strength for the material.

The minimum stress is determined as follows: Assuming that strain is linear in the plastic region and that all the plastic material is forced into compression at zero load, the residual stress would correspond to that described by the difference between the maximum strain and the nominal yield strain for the material. In this case (assuming modulus of elasticity E = 10,000,000 psi*), it would correspond to 0.010 in./in., minus 0.0075 in./in., for a residual stress of 25,000 psi.

Figure 6A shows the same loading as shown in Figure 5A; however, this represents conditions after one application of the high load. The stress cycle will now be from -25,000 to +15,000 psi for a life in excess of 10 million cycles (as found in Figure 4) for a maximum stress of 15,000 psi and stress ratio R of -25,000/15,000 or -1.66. The position for R = -1.66 is found by interpolating between R = -1 and R = -2, which would extend beyond the graph given in Figure 4. Note that this lifetime far exceeds the original value of 150,000 cycles prior to high loading. Similarly, the new life for 15,000 psi nominal stress loading will now be 50,000 cycles, rather than the original 28,000 cycles. This is shown in Figure 6B.

From the above, it will be seen that the high loads in the spectrum would tend to increase the fatigue life of a structure. This would be the case where the stress at the notch is unrestrained. However, introduction of rivets, bolts, or other fasteners tends to impede the stress at the concentration. In the case of a rivet, it could be expected that the stress would be prevented from returning to zero, even for completely reversed loading. This stems from the fact that the rivet swells on driving, tending to expand the hole, so that stress at the concentration would behave as though it were cycling at R = +0.3, +0.4, or more. At the same time, the load cycle might be at a stress ratio of zero or even a negative value.

An analogy of the stress at the edge of a hole containing a tightly driven rivet appears in Figure 7. Figure 7A shows the stress cycle at an open hole, as represented by the deflection of a spring. Figure 7B shows the spring subjected to the same loading as before; however,

---

* A value of E = 10,000,000 is used to simplify computation. This will be used throughout the remainder of this report.

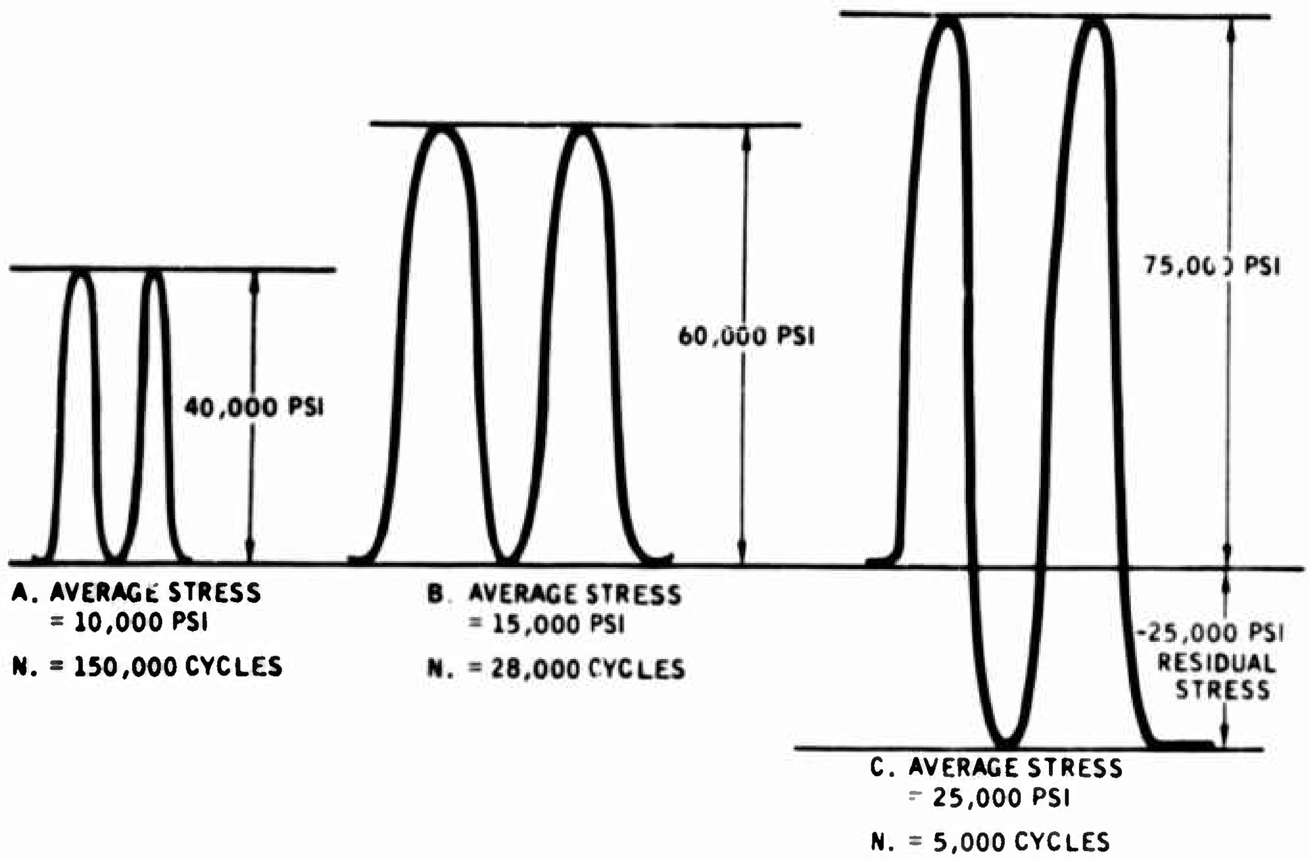

Figure 5. Stress Cycles at the Concentration for Specimens Having K_t = 4

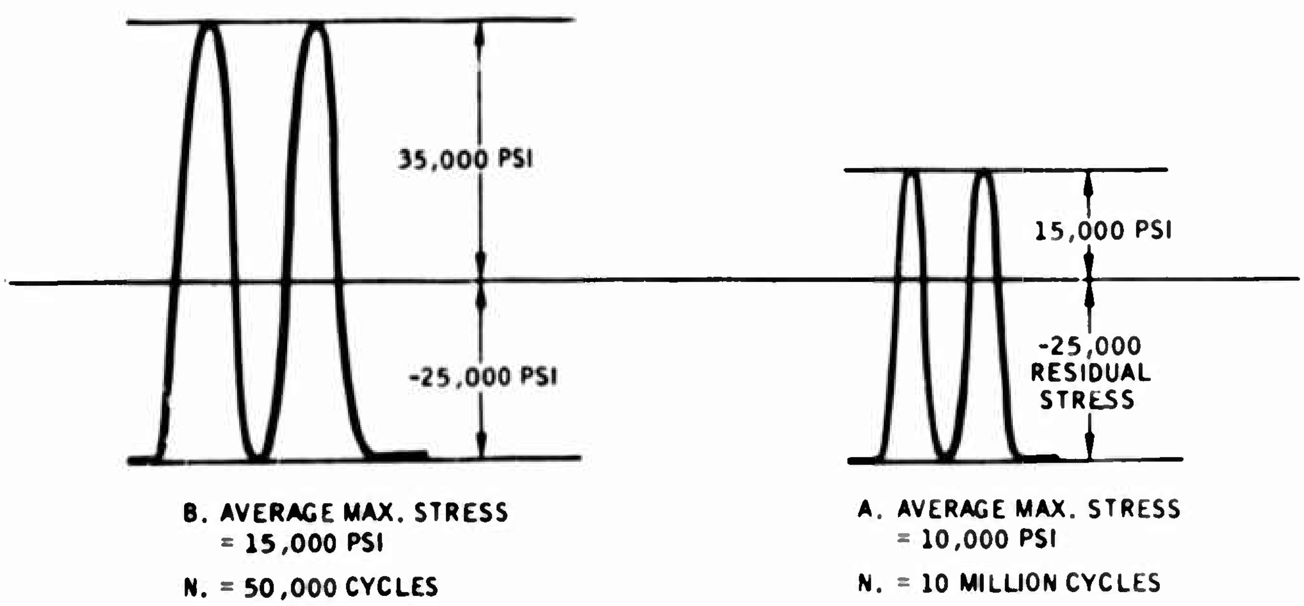

Figure 6. Stress Cycles at the Concentration for Specimens Having K_t = 4 -- After High Loading

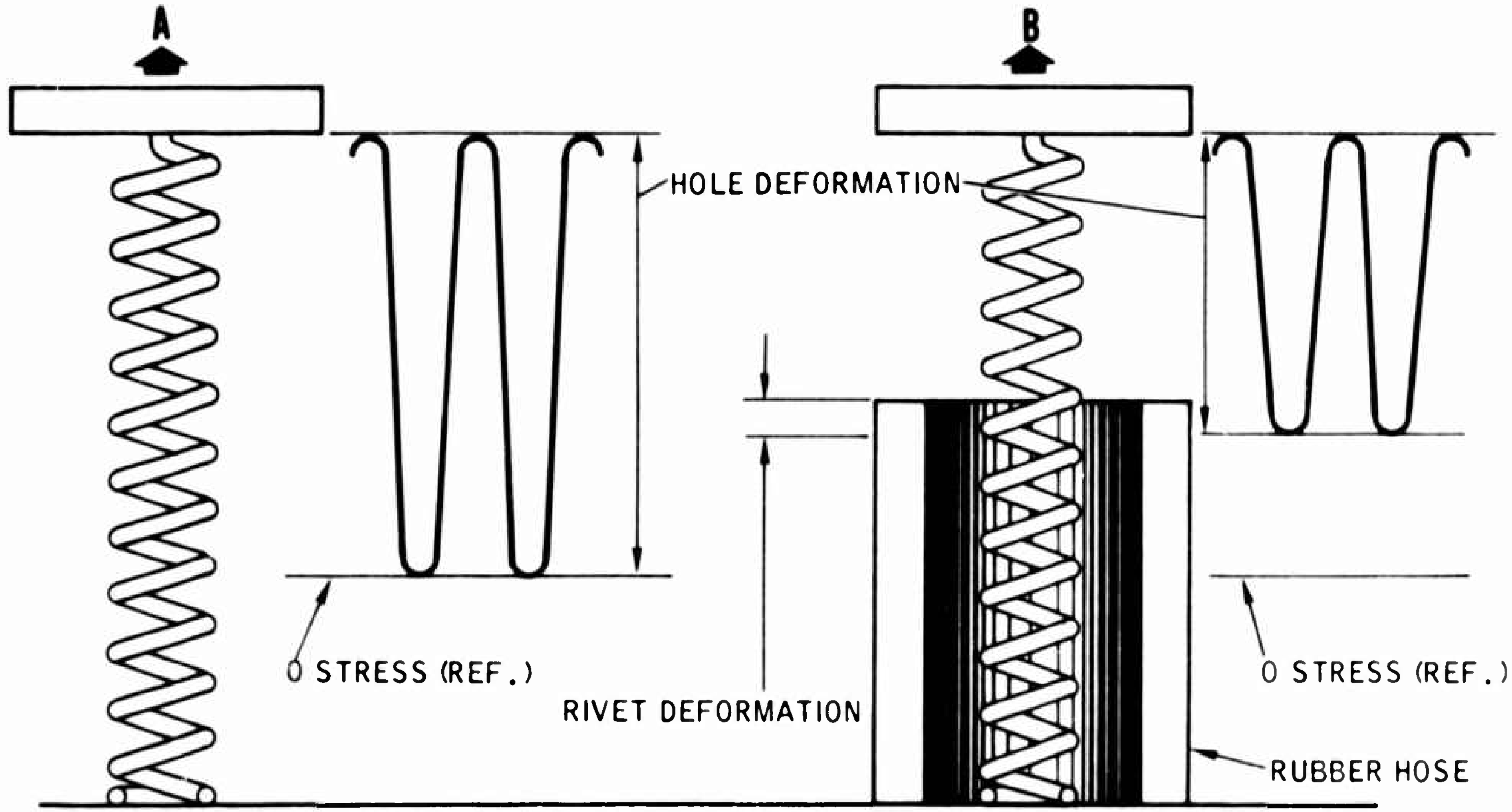

Figure 7. Spring Analogies of Stress Cycles at Edge of Open Hole, and at Edge of Rivet-Filled Hole

the bottom of the cycle is impeded by a rubber hose, preventing the return to zero. Note that the hose segment has no influence on the maximum deflection. Overloading of an amount that would cause the spring to experience permanent set should lessen the propping effect by the amount of permanent set.

Finally, where overloading causes permanent set equal to the propping effect, propping benefits in fatigue life would be lost. However, while benefits due to propping may be lost, gains in residual stress would tend to improve fatigue life. Referring again to Figure 4, for example, if the rivet propping were such as to cause the stress cycle to behave as though loaded at R = +0.5 at the 60,000 psi maximum stress, a permanent set of 0.003 in./in. would be required to relieve all propping effect. If all permanent set could be retained as a residual stress, subsequent cycling would be ±30,000 psi for a lifetime of 55,000 cycles — as compared with more than 100,000 cycles prior to overloading, or 28,000 cycles without either the propping effect or the residual stress.

Should overloading introduce a residual stress of -40,000 psi, a new life of 180,000 cycles may be found on the curve for R = -2 at a maximum stress of 20,000 psi (Figure 4). Accordingly, one could expect to find small amounts of overloading in riveted structures to be detrimental, while large amounts would be beneficial.

An example of this is given in Figure 8, where S-N curves for riveted lap joints of 7075-T6 are presented. The center curve represents the conventional S-N curve for a two-rivet lap joint. The lower curve is for similar joints, except that they were statically preloaded to 18,000 psi on the basis of nominal gross stress prior to fatigue testing. Again, the upper curve is for similar joints that were statically preloaded to 35,000 psi prior to fatigue testing.

This would indicate that behavior under spectrum-type loading would largely be dependent on the magnitude of the highest loads in the spectrum. While it is commonly thought that high loading would be always beneficial, the curves shown in Figure 8 would indicate that this is not the case. In fact, spectrum-type tests on identical joints gave Σ n/N values of about 0.23 if the highest load was 18,000 psi. Spectrum loading on joints that were preloaded to 35,000 psi gave Σ n/N values in excess of 100, after which testing was discontinued.[10] The reason is that 18,000 psi preloading was just enough to take away the propping effect without introducing beneficial residual stress such as accompanied the 35,000 psi preloading.

In addition to magnitude, the order in which the highest loading occurs is also important. Where fatigue life is improved by high loading, the spectrum life will be greatest when high loading occurs early. On the other hand, where spectrum block size is small — so that at least 100 blocks are sustained prior to failure — one would expect that order of loading would make no difference. The exception to this would be where the highest load introduces more residual stress than can be retained over the duration of one sequence. In this case, life will be greater where low loading immediately follows the highest load in the sequence. This stems from the fact that the residual stress is more beneficial at low loads than at intermediate loading. Thus, increase in spectrum life can be expected where low loads are applied before the residual stress has a chance to relax.

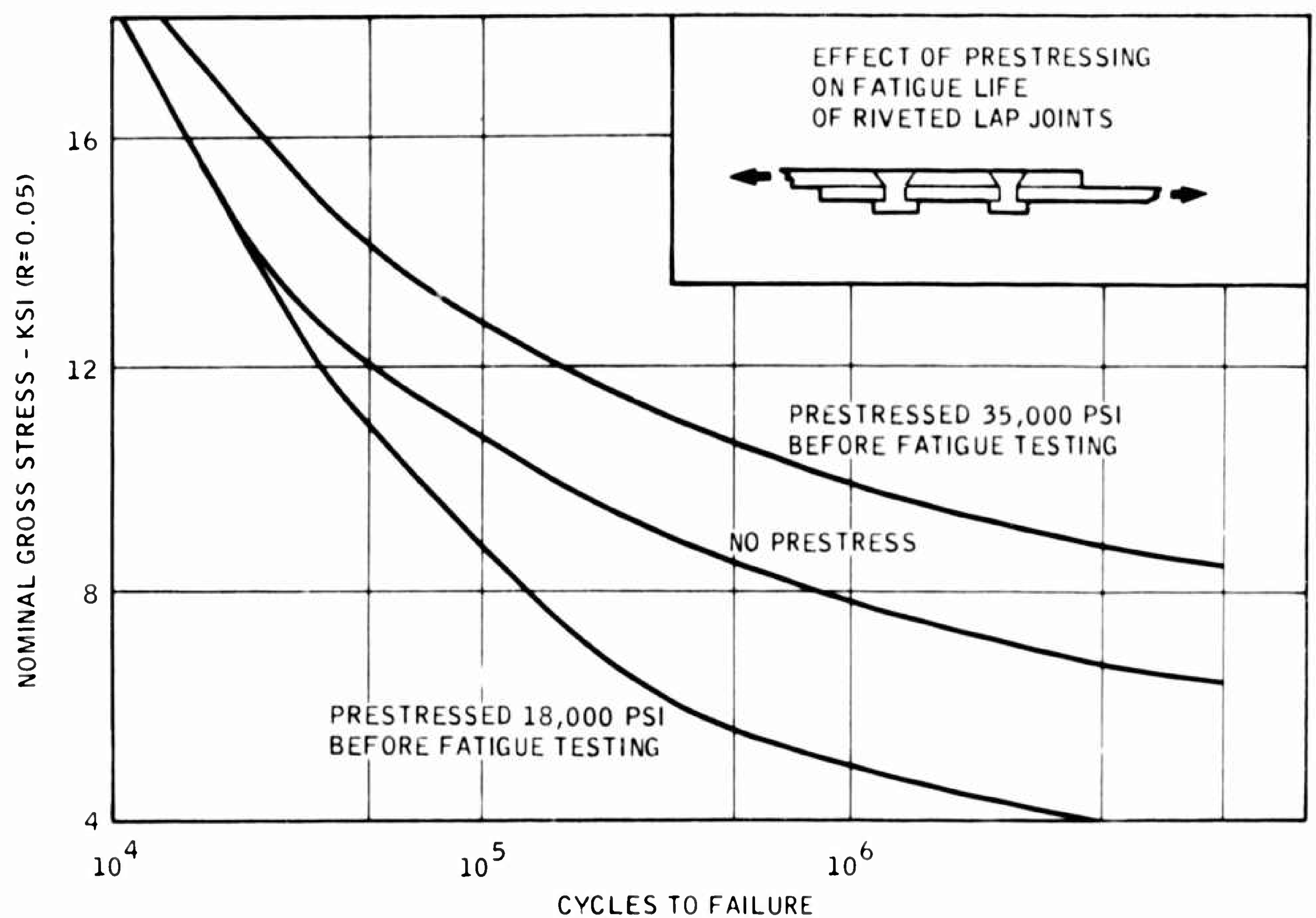

Figure 8. **S/N Curves for Riveted Lap Joints With Various Preloads**

SECTION III

THE SMITH METHOD

As in the Linear Strain Theory, the Smith Method considers the stress at the concentration and uses S-N curves of smooth specimens for estimating fatigue life. Whereas the Linear Strain Theory employs theoretical stress concentrations in conjunction with strain for obtaining stress at the concentration, the Smith Method requires two things only:

1. A single datum point for a structure loaded at a constant amplitude wherein failure occurs at a lifetime which is shorter than that for a smooth specimen cycled at R = 0 and a maximum stress equal to the material's yield strength.

2. S-N data for smooth axially loaded specimens of the material from which the structure was fabricated.

STRESS AT A CONCENTRATION

A smooth axially loaded specimen of 7075-T6 aluminum alloy, when subjected to repeated tension loading (R = 0), can sustain maximum stresses amounting to the yield strength of the material for a lifetime of about 10,000 cycles.

Although higher stress amplitudes can be sustained in smooth specimens for shorter lifetimes, they cannot be obtained without considerable elongation — 6 percent in the case of 7075-T6 aluminum alloy at 80,000 psi for a lifetime of 3,000 cycles, as shown in Figures 1 and 9.

In a structure, however, the material at a concentration cannot acquire such elongation without also yielding the material in the adjacent area. This would lead to the conclusion that the maximum stress (at a concentration) in a structure cannot substantially exceed the yield point so long as nominal stresses are below yield for the material. In a structure having a concentration factor of 3, the maximum strain at the concentration tenable without yielding the entire cross section would be about 2 percent.

Consider a 7075-T6 aluminum alloy structure having a stress concentration of 3 and subjected to loading at R = 0 such that the maximum strain at the concentration is 2 percent. While 2 percent strain (of which at least 1.2 percent is plastic) should be sufficient to introduce a residual stress equal to the yield strength for the material, let's assume that only 90 percent of yield is introduced as a residual compressive stress (R = -0.9). This gets away from having to worry about the Bauschinger effect and does not materially affect the final results.

According to the stress-strain curve in Figure 1, a strain of 2 percent would correspond to about 77,000 psi stress. Since we assumed a residual compressive stress of 90 percent of this amount (R = -0.9), the actual stress cycle would have been defined by R = -0.9 and a maximum stress of 77,000 psi. In Figure 9, a straight line is drawn from the intersection of R = -0.9 and 77,000 psi to the intersection of R = 0 and the nominal yield value for the material (74,000 psi). The shaded area above this cutoff line represents maximum stress values, which have just been shown to be inapplicable to a structure having stress concentrations.

The principle would be the same, irrespective of the stress concentration factor, except that lower concentrations may not introduce so much residual stress. Lessening the concentration would limit the amount of maximum strain available at the concentration without yielding the base area. This would more or less limit the amount of residual stress. Since the maximum stress is also limited, the position of the cutoff line would not be materially affected. For example, a point representing a maximum stress of 75,000 psi and a stress ratio of -0.5 would still fall on the original cutoff line. Such a stress condition would be tenable in a structure having a concentration of between 1.6 and 1.8. The method, as presently conceived, is not applicable for structures of lower concentrations.

Higher concentrations, while permitting larger amounts of strain, would be unlikely to introduce greater amounts of residual stress than the compressive yield of the material — at least, they could not be sustained for any length of time without relaxing. Therefore, the cutoff line would likely fall along the S-N curve for R = -1, which flattens out considerably at the higher stress values, so that the final position of the cutoff would be about the same as shown for a concentration factor of 3.

Looking at the slopes of the curves in Figure 9, it is readily seen that, whatever the concentration, the cutoff line established for a stress concentration of 3 is unlikely to differ enough from those of other concentrations to have a distinguishable influence on fatigue life predictions.

The purpose of the cutoff line is (1) to establish the maximum stress, (2) to find the minimum stress as determined by the product of the stress ratio, R, times the maximum stress, and (3) the stress range, which is the absolute sum of the maximum stress and the minimum stress. The minimum stress is found by the intercept of the cutoff line and the R curve for the given lifetime.

Generally, it will be necessary to interpolate between the various values of R to estimate the correct amount of residual stress. For example, were a structure to fail after 2,000 cycles of loading at R = 0 (based on load cycle), the intercept would be at 75,000 psi maximum stress and an interpolated R of about -0.55 for a minimum stress of -41,000 psi. See Figure 9.) Knowing the maximum stress, minimum stress, and stress range, it is now possible to predict the fatigue life of a similar structure for any other load or combination of loads for simulated service testing.

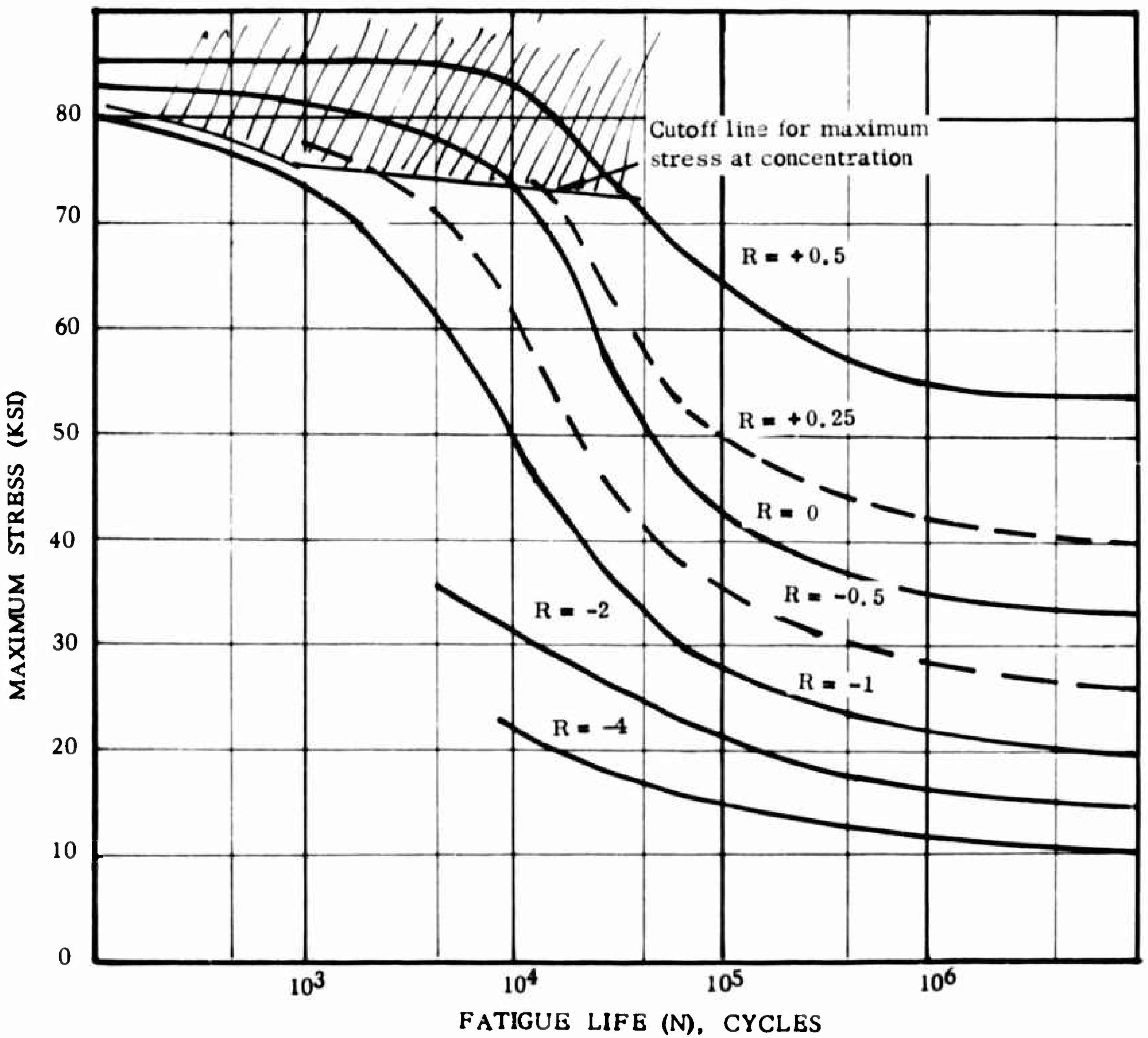

Figure 9. S-N Curves for 7075-T6 with Maximum Stress Cutoff

STEPS IN THE SMITH METHOD

Although the above example was illustrated on 7075-T6 aluminum alloy, the principle should apply to any alloy if the following steps are observed:

1. On a stress-strain curve for the material, find the stress corresponding to 2 percent strain.

2. On a family of S-N curves of the material, mark a point on the curve for R = -1 corresponding to the stress found in Step 1*.

3. From the point found in Step 2, draw a straight line to intercept the curve for R = 0 at a stress representing the nominal yield strength for the material.

4. Find the R curve that coincides with the intersection of the line drawn in Step 3 and the number of cycles representing the lifetime of a structure subjected to a constant amplitude loading. The minimum stress in the loading cycle is the product of R and the maximum stress, both of which are found at this intersection. (It is assumed that the structure failed at less than the number of cycles corresponding to the intercept of the yield strength and the S-N curve for the material at R = 0).

5. Adding the absolute values of the minimum and the maximum stresses gives the stress range (stress amplitude). This is the value used for estimating fatigue life at other loads and is extremely important.

6. Stress amplitude (range) can then be prorated for any other load in the spectrum for which lifetime is desired, giving consideration to the effect of high loading in the spectrum. For a structure loaded at R = 0, the maximum stress for any load is in direct proportion to the stress amplitude found in Step 5, except where the proportioned amplitude is greater than the yield strength for the material, in which case the amount of stress greater than yield will be treated as a residual stress and the fatigue life will be found directly from the S-N curve whose stress ratio corresponds to the ratio of the residual stress divided by the yield stress.

---

* R = -1 is used here because it is easier to identify than R = -0.9 as used earlier. This will not affect fatigue life estimates, since the maximum stress is about the same for both. This should not be construed to mean that the value of R is unimportant, since very large differences in minimum stresses are found at corresponding lifetimes.

7. Where the residual stress from a preceding high load is greater than for the load at hand, use the larger value except for the first time through the sequence. In an ascending test spectrum, the cumulative damage may be considered as $\Sigma\ n/N = 1 - d$ where d is the fractional damage acquired during the first sequence, or during the time spent prior to high loading. Values of N in all cases are estimated from S-N curves for smooth axially loaded specimens, using the above procedure.

SECTION IV

TEST PROGRAM

The ultimate objective of any method for predicting fatigue life is to predict the fatigue life of a structure for simulated service loading. The present test program was designed with this objective in mind. Other works[18] have shown that a typical riveted joint could experience both gains and losses in fatigue life for spectrum loading. This depends largely upon the manner of loading and the magnitude of the highest load in the spectrum. It was felt that losses in fatigue life were largely the result of loss in rivet propping action, and that subsequent gains resulted from beneficial residual stresses as explained by the Linear Strain Theory. Since riveting is largely dependent upon individual workmanship, it was felt that a riveted structure would contain too many variables to illustrate the appropriate factors.

Accordingly, a simulated structure in the form of a lug with a theoretical stress concentration factor of 3.6 was used in this program. A tapered bolt was used to transmit the load so that various amounts of interference would simulate rivet swelling. This specimen possessed the particular advantage of permitting control over the amount of interference. The lug specimen is illustrated in Figure 10.

Since one purpose of the program was to associate the relationship between the fatigue life of notched specimens and that of smooth specimens, ten-inch radius specimens were prepared from the same sheets of material used for the notched specimens. A typical specimen is shown in Figure 11. The test program was planned to illustrate the following parameters:

1. Basic fatigue strength of material for axial loading

2. Fatigue strength of notched specimens with no propping effect

3. Fatigue strength of notched specimens with propping effect

4. Effect with preload on propping effect

5. Effect of preload on residual stress

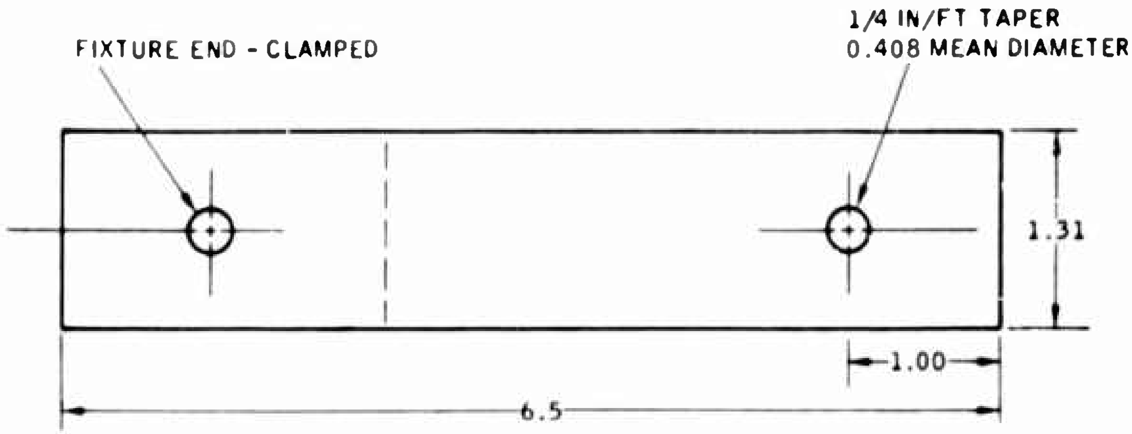

Figure 10. Lug Specimen

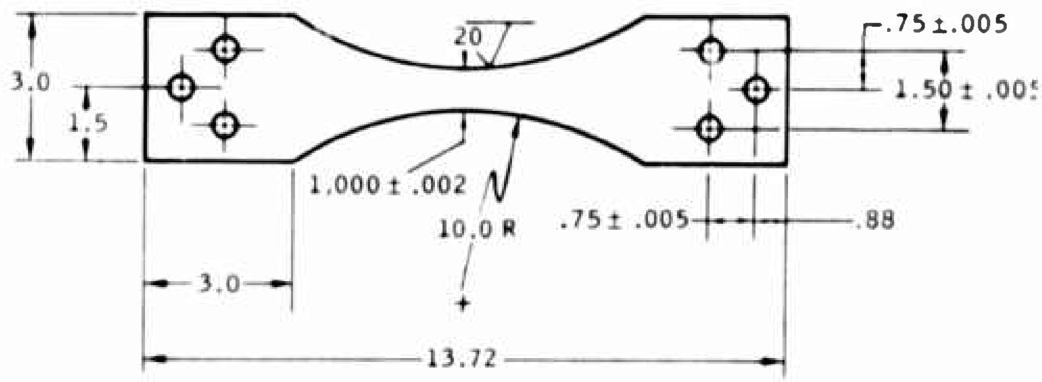

1. THERE ARE TO BE NO NICKS, SCRATCHES, OR UNDERCUTS IN THE TEST SECTION.
2. ℄ OF CENTER HOLES TO BE ON ℄ OF TEST SECTION WITHIN .002 T.I.R.
3. FINISH TEST SECTION BY LONGITUDINALLY POLISHING WITH 0 THRU 000 EMERY.

Figure 11. Smooth Specimen

6. Cumulative damage test showing

   a. Effect of propping spectrum life

   b. Effect of residual stress on spectrum life

   c. Effect of load deletion on spectrum life.

In all cases, special care was exercised in finishing the edges of the smooth specimens: a mill bastard file was used first to break corners, followed by a 150-grit emery cloth for finishing. All polishing operations were in the direction of the specimen longitudinal axis. Previous experiments have shown that finishing in this manner provides the same fatigue life as that obtained for specimens having a final buffing.

FIXTURES

The lug specimen was tested in a special fixture that clamped the tapered bolt in a position to prevent the specimen from rubbing against the side of the clevis. (See Figure 12.)

A special fixture for compressively loading the smooth specimens was designed to prevent lateral buckling, yet not restrain axial loading (Figure 13). Axial load fatigue properties were determined in either a Sonntag SF10U (10,000 lb) or 20U (20,000 lb.) fatigue testing machine. Both machines are of the constant-load type. In the case of the 10U, dynamic load is introduced by centrifugal force and mean load by a spring automatically monitored by an electronic preload maintainer. The SF20U supplies dynamic force through a vibrating mass excited by a small eccentric. Loading is monitored by a strain gage load cell incorporated in the machine with an Ellis BA12 amplifier and a cathode ray osscilloscope for visual checking.

Lug specimens were tested in a Sonntag SF1U (2,000 lb) fatigue testing machine. This machine operates on the same principles as the 10U machine described above.

Since one purpose of the program was to determine the effect of high loads upon the subsequent lift of notched specimens, S-N curves were developed for various stress ratios and amounts of preloading. Spectrum tests were performed in a Tatnall-Budd hydraulically operated fatigue testing machine capable of step or random loading for 12 values. Each load is governed by a preset value at any one of the load channels. Load is controlled by a function generator signal to a hydraulic servo valve. A strain gage dynamometer is part of the closed-loop system to maintain the load for all levels.

A schedule for spectrum loading is presented in Figure 14.

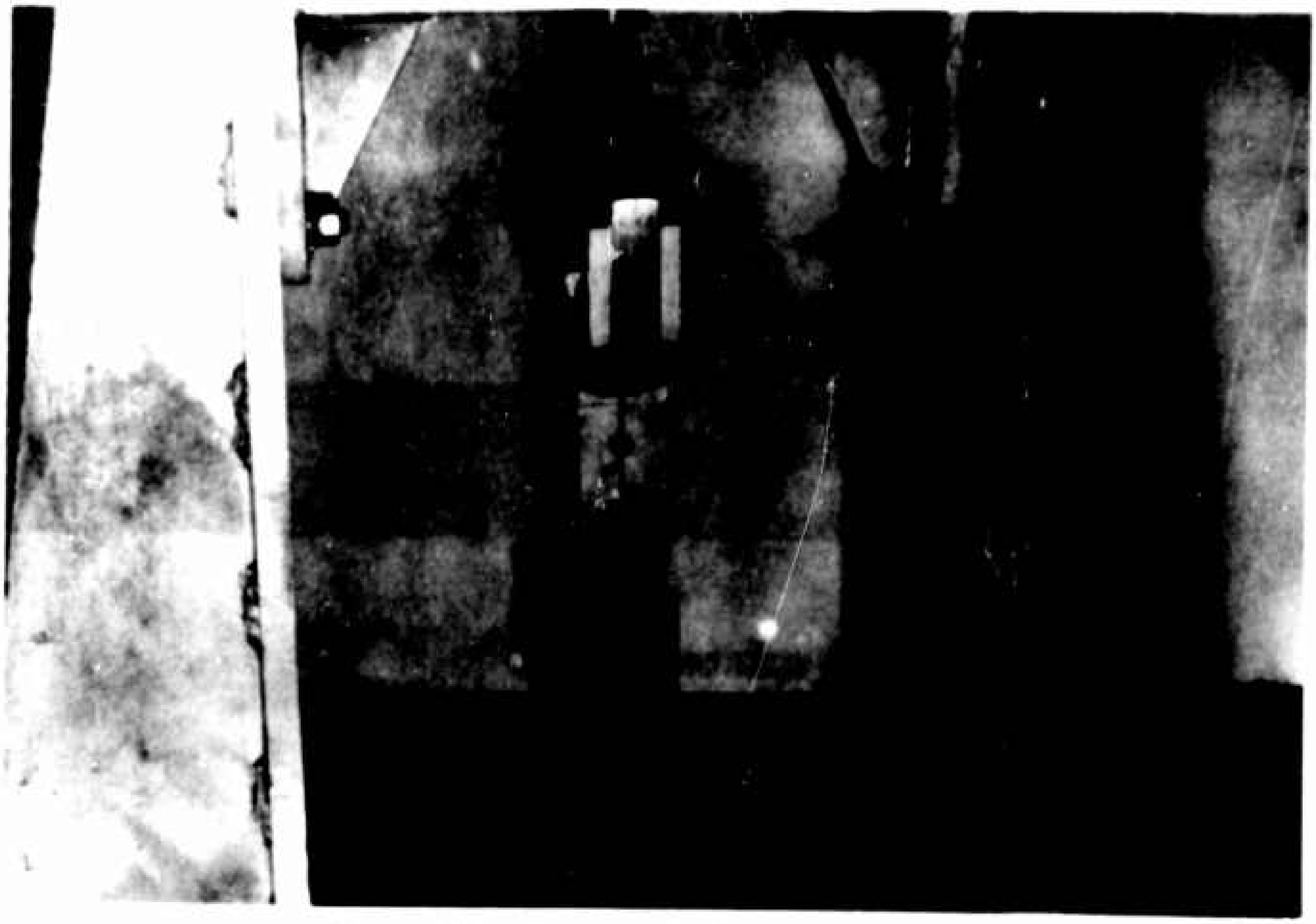

Figure 12. Fixture for Lug Specimens

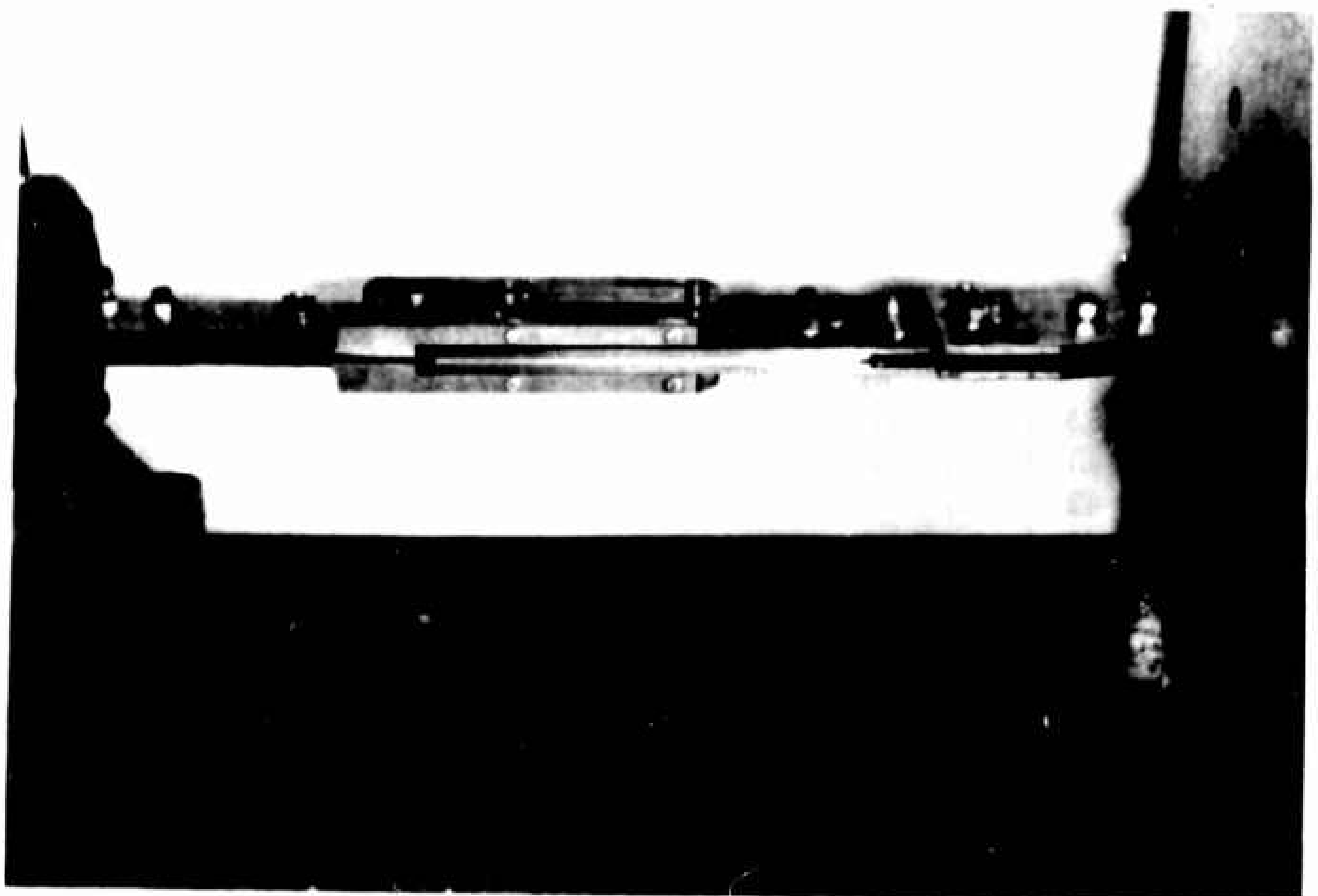

Figure 13. Lateral Support Fixture for Smooth Specimens

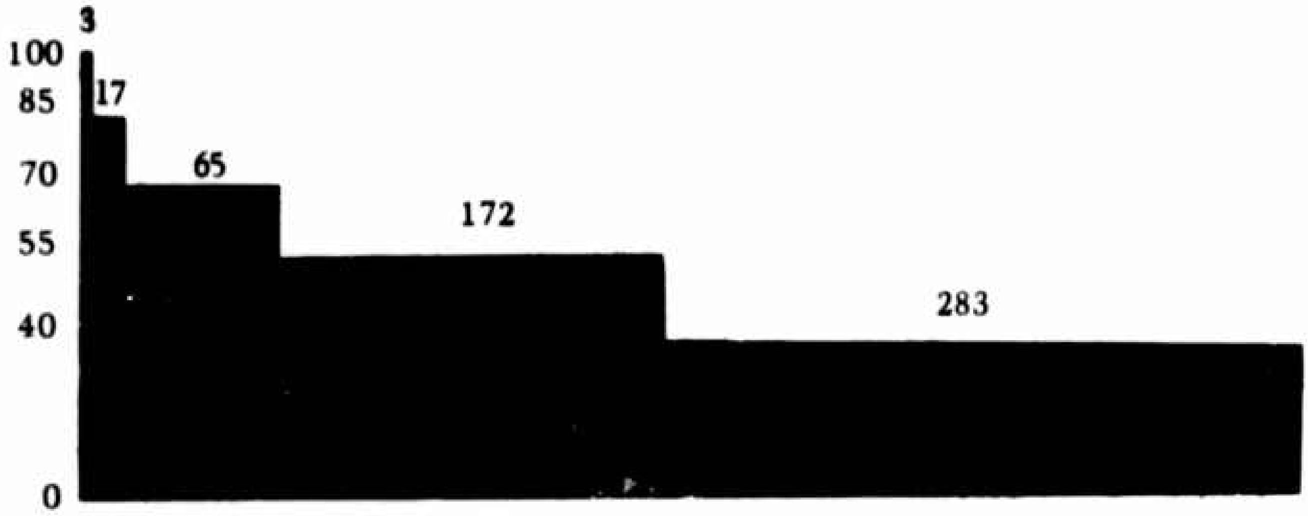

SPECTRUM II

LOAD SPECTRA
CYCLES PER SEQUENCE

LOAD CONDITION: Descending Loads Per Cent*		I	II	III	IV	V	Ascending Loads Per Cent	
Notched	Smooth						Notched	Smooth
100	100	3	3		750	750	30	42
85	94	17	17		283	283	40	45
70	86	65	65	65	172	172	55	53
55	53	172	172	172	65	65	70	86
40	45	283	283	283		17	85	94
30	42	750		750		3	100	100

* 100% = 40,000 psi for lug specimens
= 48,000 psi for center hole specimens
= 79,000 psi for smooth specimens

Figure 14. Schedule for Spectrum Loading

TEST RESULTS

Test data are presented in Tables I through XIII in the Appendix, and constant level S-N curves are presented in Figures 4, 9, 15, 16, 19, and 20. Results of spectrum tests are summarized in Figure 17, where average test results and predicted values are plotted on a log-log scale. The heavy diagonal line represents the case where predicted and test values are equal. Those points falling above the diagonal line represent predictions that fall short of test lives, while whose below the line represent cases where predictions exceed test lives.

The basic premise the Miner relation is valid if used in conjunction with true stress is represented by results of the spectrum tests on smooth specimens (see Table XIII), which are plotted in Figure 18 with the symbol +. Although the amount of scatter in Figure 18 conforms with that normally found in fatigue tests, the average $\sum n/N$ amounts to about 1.04--this for descending loads, which other researchers[9] have found to yield $\sum n/N$ values substantially less than 1.

Predictions of fatigue life for lugs made by the Linear Strain Theory are represented by triangles and those by the Smith Method are represented by circles. Blackened circles and triangles represent specimens loaded with tapered bolts having 0.003-inch interference (bolt diameter 0.003-inch larger than hole). Here, it will be seen that fatigue life exceeded predictions by substantial amounts--especially in the case of 2024-T3. Theoretically, the high loads in the spectrum should have relieved all of the propping effect so that the spectrum life should not have differed from lives for lugs with no interference. Results of experiments made to determine effect of preloading on subsequent lives are given in Table IX. Where prestressing amounted to 40,000 psi or more, little difference is shown between the lives of lugs with interference, and those without, thus agreeing with theory. The fact that greater than theoretical values were experienced with interference fasteners indicates that a factor other than propping was instrumental in prolonging life for spectrum loading--perhaps frictional forces during load change. This is substantiated to some extent in that 2024-T3 material is harder to drill than 7075-T6 because of seizing, which prohibits easy clearance of drill shavings. This facet was beyond the scope of this investigation.

Figures 19 and 20 show graphs for loading at $R = +0.5$ for lugs having no interference and $R = 0$ for lugs having 0.003-inch interference. By definition, the intersections of these graphs should represent one-half of the maximum nominal stress due to interference. Considering that the stress concentration was 3.6, this would mean that the stress due to interference was about 40,000 psi.

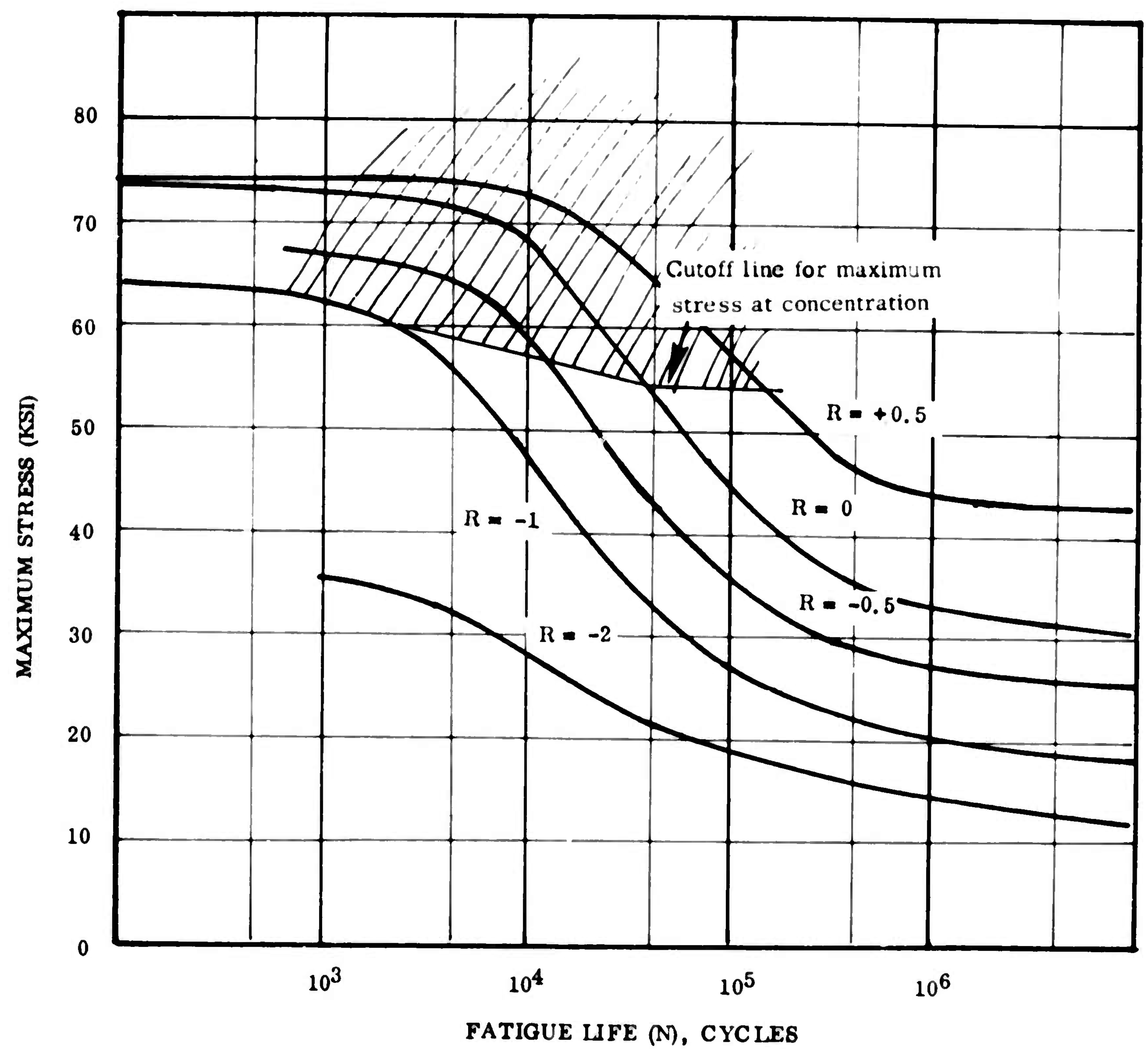

Figure 15. S-N Curves for 2024-T3 Aluminum Alloy Sheet

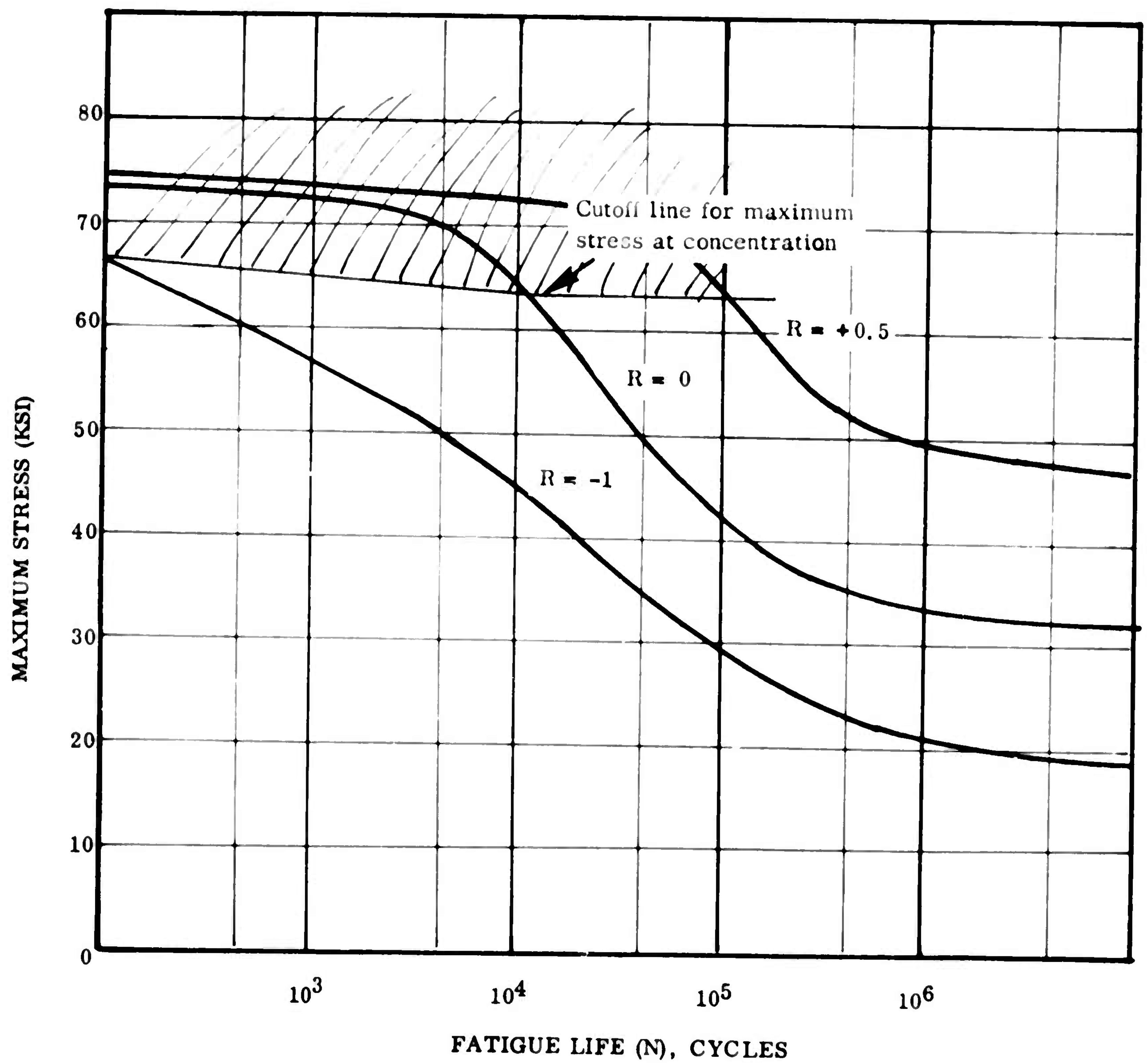

Figure 16. S-N Curves for 2024-T81 Aluminum Alloy Sheet

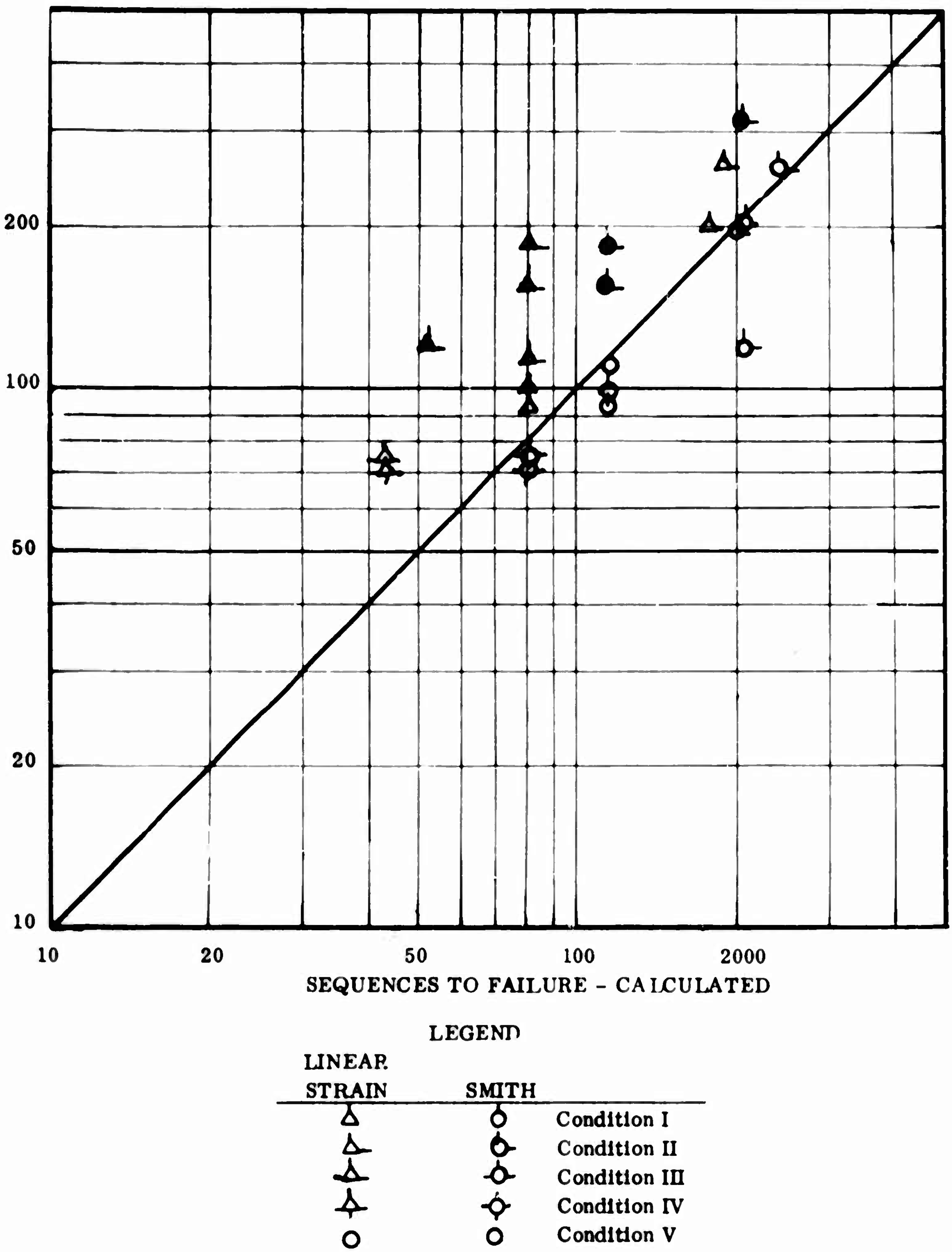

Figure 17. Comparison of Spectrum Test Results with Predicted Lives of Notched Specimens by the Linear Strain and Smith Methods

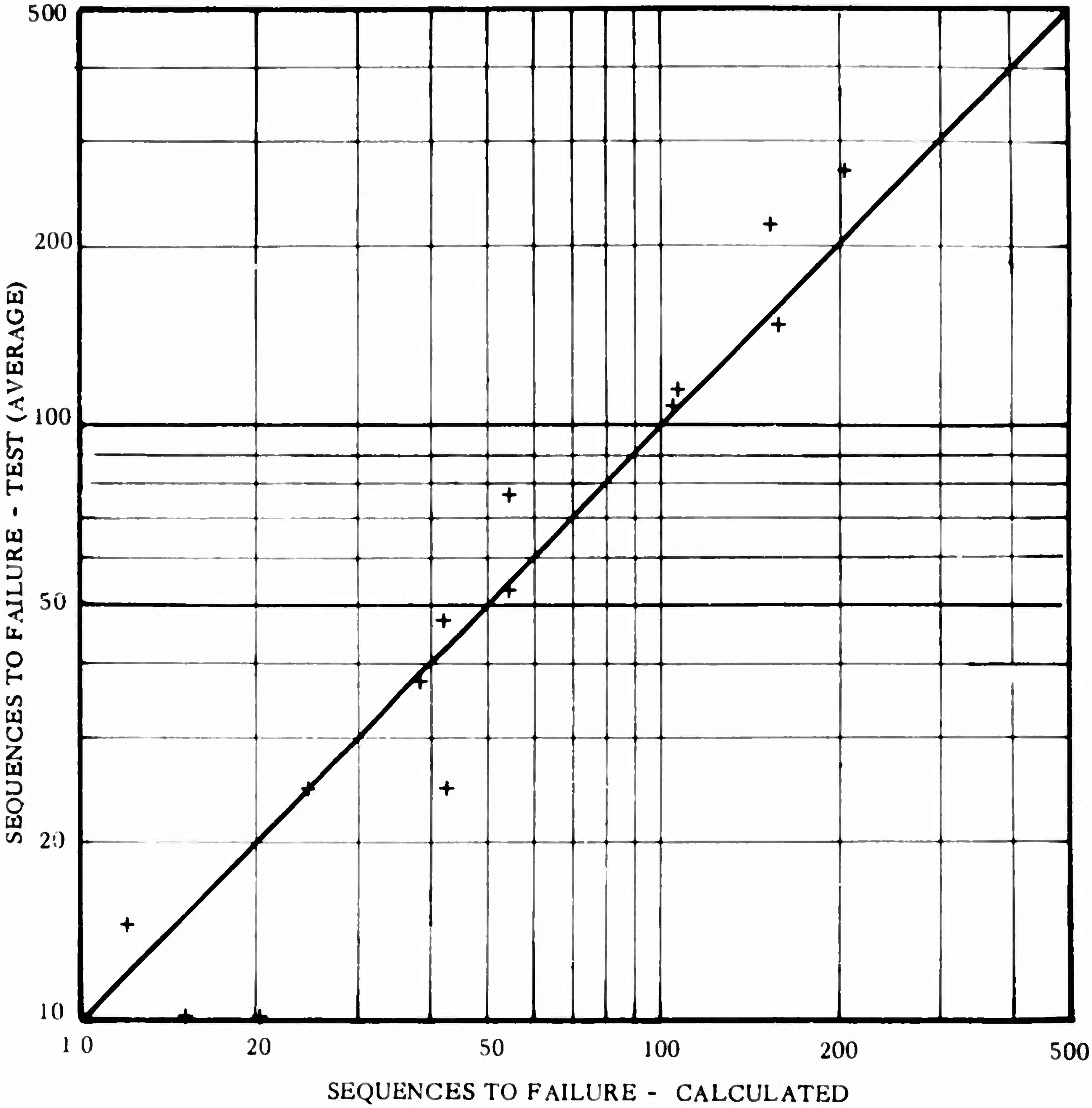

Figure 18. Comparison of Spectrum Test Results with Predicted Lives of Smooth Specimens

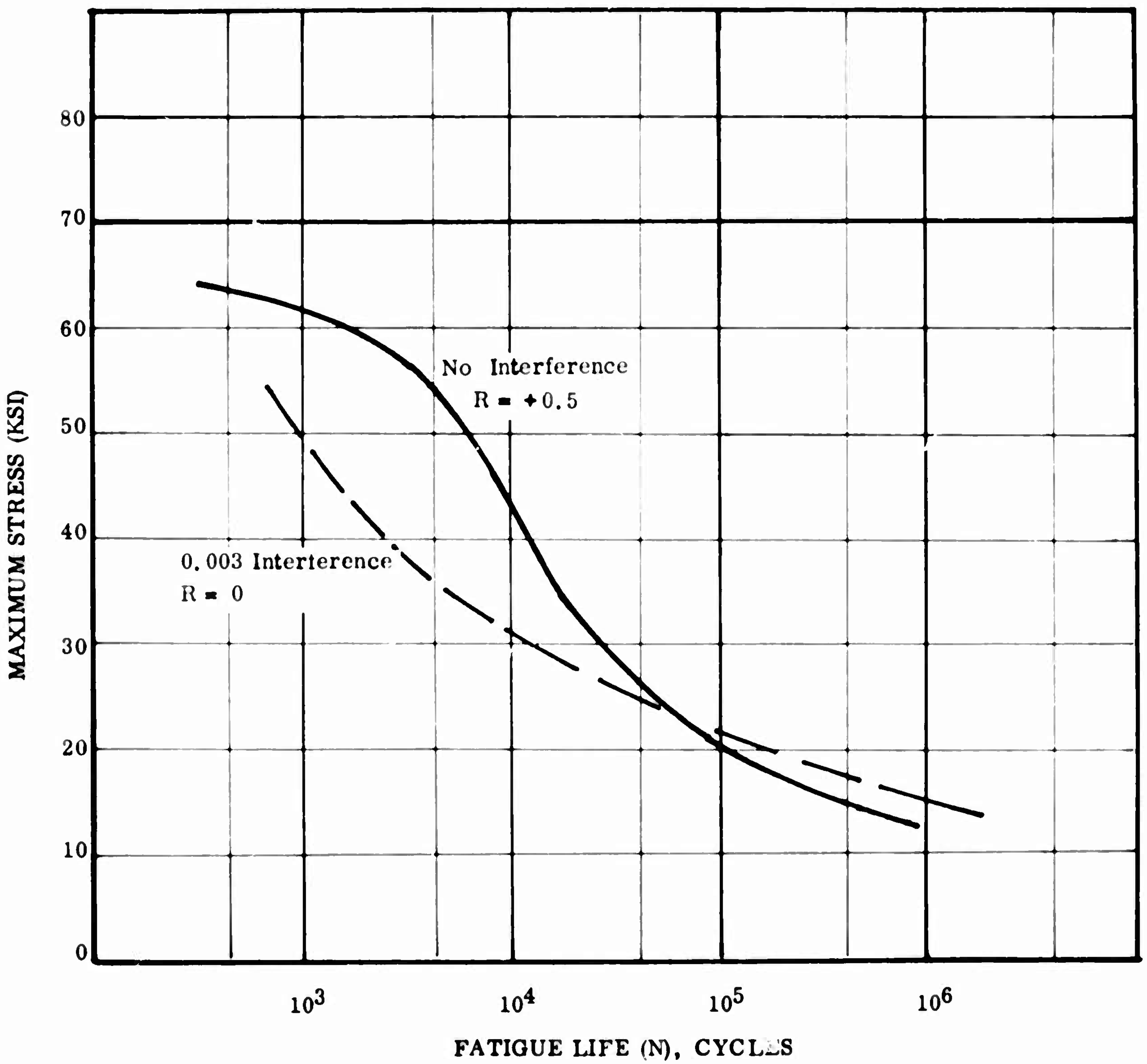

Figure 19. S-N Curves for 7075-T6 Lugs--Stress Due to 0.003-Inch Interference is Indicated by Intersection of Curves

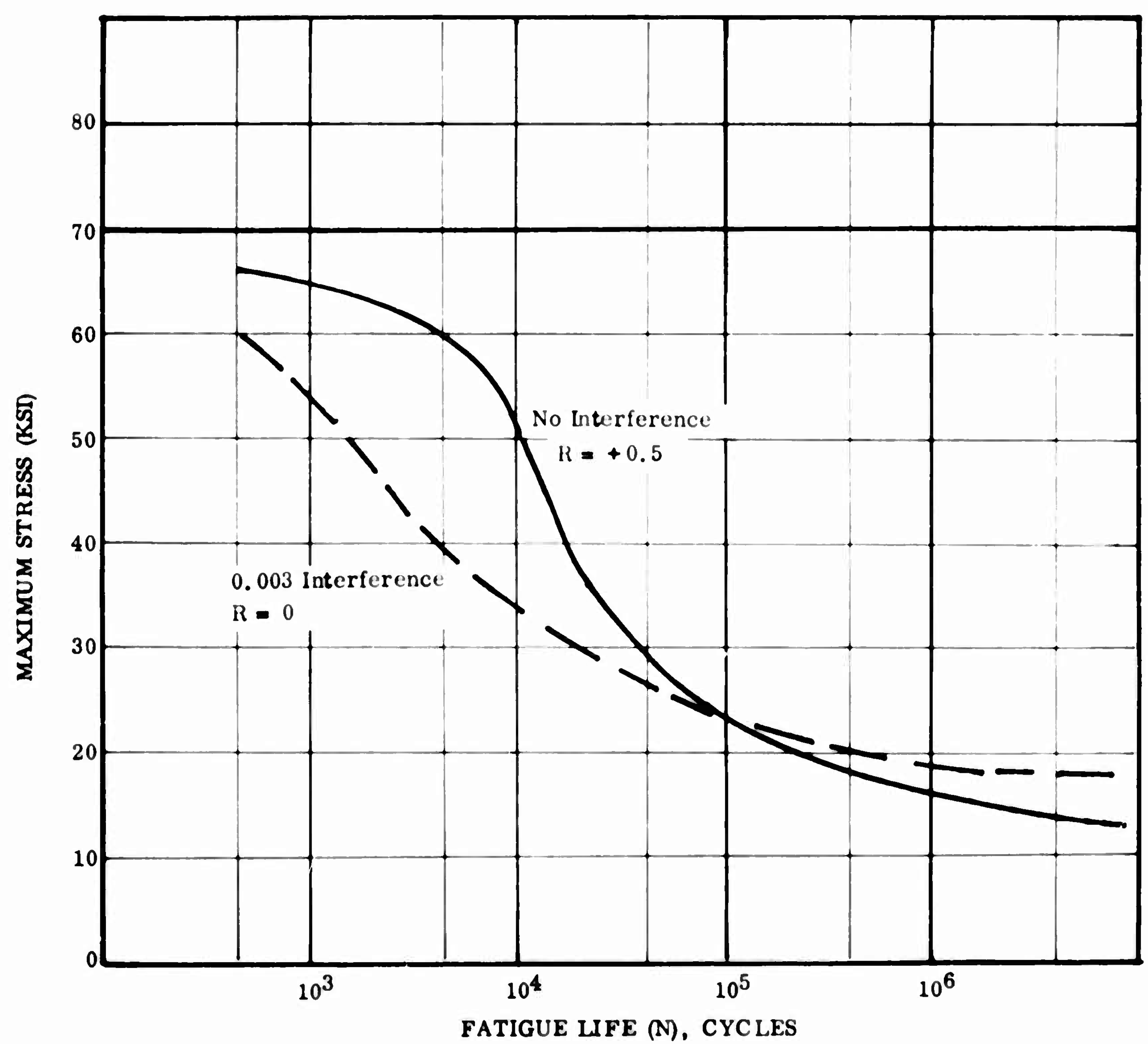

Figure 20. S-N Curves for 2024-T3 Lugs--Stress Due to 0.003-Inch Interference Indicated by Intersection of Curves

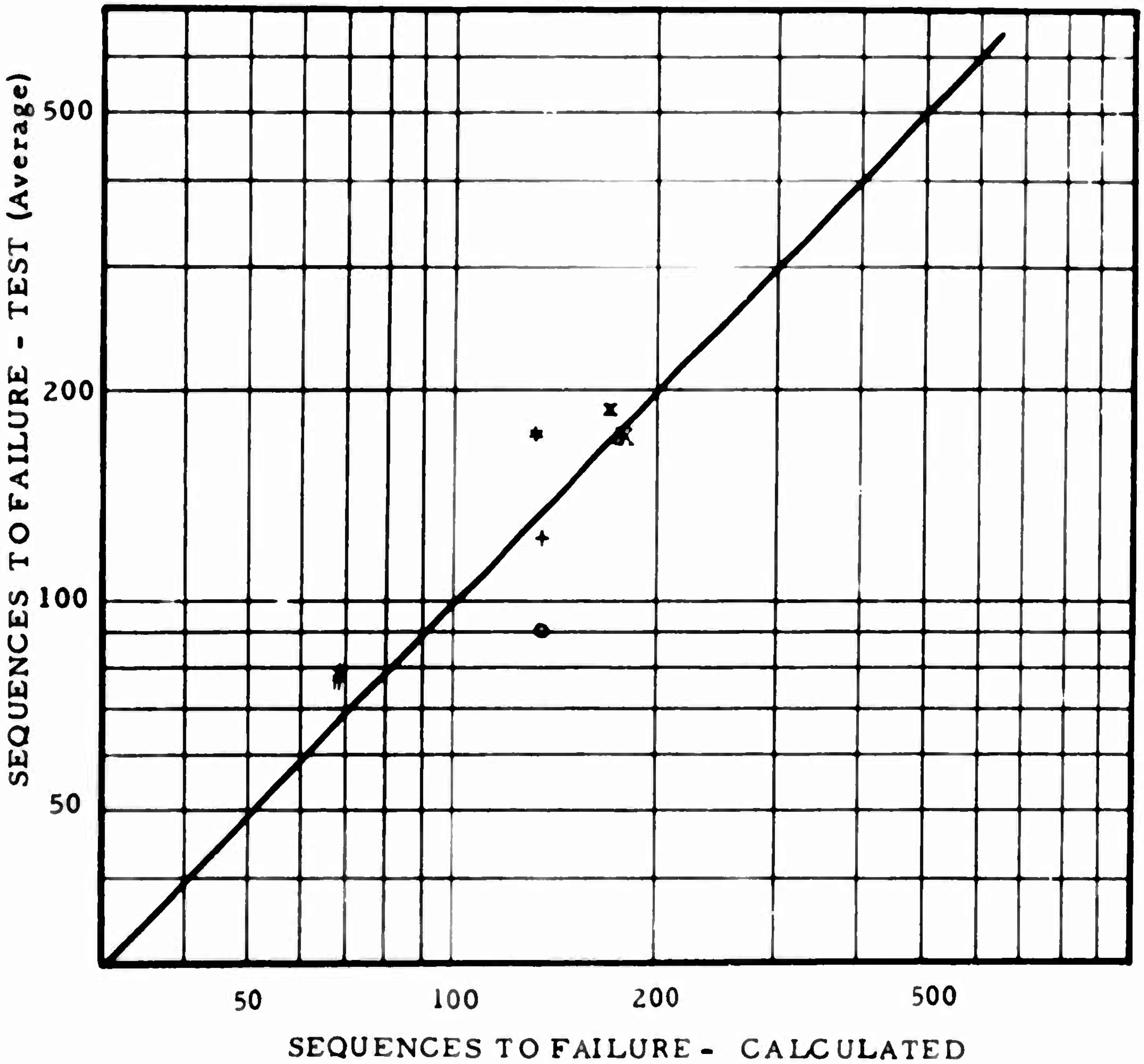

LEGEND:

+ Condition I, Horizontal Stabilizer
* Condition II, Horizontal Stabilizer
o Condition III, Horizontal Stabilizer
Condition IV, Horizontal Stabilizer
x Random on Wing
X Lo-hi on Wing

Figure 21. COMPARISON OF CALCULATED TO TEST VALUES FOR NAVY FULL SCALE TESTS

SECTION V

CORRELATION BETWEEN THEORETICAL & TEST RESULTS

While there is a high positive correlation between theoretical and test results, it is of interest to note that predictions made by the Linear Strain Theory usually fall short of actual test life, while those by the Smith Method exceed test values. This is especially true in the case of 2024-T3, where the Linear Strain prediction is substantially less than the value found by testing, while the Smith prediction exceeds the test value for condition 1 by 1.5. This is true to a smaller extent with 7075-T6. Such divergence indicates that the correct answer lies somewhere between the two methods. Two possible reasons for this are:

1. Theoretical stress concentration is too high -- perhaps a Neuber* value should be used. This would raise the Linear Strain predictions, but would not affect predictions for the Smith Method.

2. Too much residual stress was assumed in the Smith Method. While the residual stress estimated by the Smith Method could be retained for the duration of one cycle, the retention for the duration of a sequence is questionable -- in fact, this appears to be the reason why the spectrum life for an ascending spectrum was greater than for the descending spectrum. Furthermore, it would appear that estimates made by assuming that all of the residual stress is retained could be unconservative for a structure having long time elapses between application of high loads.

While other avenues of exploration might be in order also, these two should suffice for the time being. First, let us try correcting the predictions on 2024-T3 lugs -- this having the widest divergence between predicted and test life. Assuming first, that the divergence between test data and predictions by the Smith Method resulted from differences between (1) amounts of residual stress assumed on the basis of the short-life constant-amplitude data, and (2) the amounts of residual stress actually retained. While it would be virtually impossible to determine actual amounts, calculations can be made to show the amount of residual stress required to make predictions agree with test results.

---

*
$$K_n = \frac{K_t - 1}{1 + \frac{\pi}{\pi - \omega} \sqrt{\frac{A}{R}}}$$

where K_t is equal to theoretical stress concentration factor

ω = flank angle (ω = 0 for hole and notches with parallel sides)

R = radius of hole or at the bottom of notch

A = material constant (equals 0.02 for aluminum alloys).

Taking Spectrum No. I, the residual stress calculated by the Smith Method amounted to 50,000 psi -- which for 2024-T3 was only 5,000 psi below the tensile yield of the material. The stress range at 100 percent limit load (40,000 psi) was 110,000psi, according to the following calculations:

Nominal Stress KSI	Stress Range (KSI)	F_{max} (KSI)		F_{min}		R		N		n	n/N	
		A	B	A	B	A	B	A	B		A	B
40	110	59.5	59.5	-50	-50	-0.84	-0.84	2,800	2,800	3	0.0011	0.0011
34	93	43		-50		-1.17		10,000		17	0.0017	0.0019
28	77	27		-50		-1.85		35,000		65	0.0019	0.0028
22	60	10		-50		-5.0		10^6		172	0.0002	0.0011
16	44	-6		-50						283		

$\Sigma n/N$ = .0049 .0069

(A) Sequence to Failure $= \frac{1}{0.0049} = 204$

(B) Sequence to Failure $= \frac{1}{0.0069} = 145$

NOTES:

(A) values (uncorrected) assumes all residual stress retained.

(B) values (corrected) 42 KSI residual stress retained at all loads except first load, corresponding to a relaxation of 8 KSI.

Stress Range = (59,500 x -0.85) plus 59,500 psi.

F_{max} = maximum stress (taken from cutoff line at 2,800 cycles).

F_{min} = minimum stress = difference between stress range and maximum stress.

Results from the Smith Method, being independent of theoretical stress concentration factors, would not be changed by use of another concentration factor. In order to correct the Linear Strain method (assuming that the corrections made for the Smith Method were correct), it can be seen that the needed stress concentration K_t would be 110/40, or 2.75 instead of the K_t of 3.6 used in computation. As it turns out, the value of 2.73 would very closely approximate a Neuber value (K_n) of 2.92.

A comparison of predicted versus test life for full scale structures tested at the Naval Air Research Center, Philadelphia, is presented in Figure 19. Here excellent correlation is achieved, although no correction was made for relaxation of residual stress. Why should a correction be required in one case and not in the other? The answer would appear to be the rate of loading. While the constant level loading cycle for short life specimens was one-fifth of a second, that for the full scale structural test was half a minute or more. This points to an important generalization that might be made regarding all testing -- that accelerated laboratory tests are not necessarily valid unless due allowance is made for elapsed time of testing. This is especially true where elevated temperatures tend to relax residual stress or where load reversals tend to remove residual stresses left by previous loading. This, again, is beyond the scope of the present program.

SECTION VI

CONCLUSIONS

The high positive correlation between predicted and test data developed by this study indicate that a further investigation would likely gain even closer agreement, either by proper weighting or a similar method of adjustment. However, it is felt that the work accomplished its purpose of providing experimental data for exploring relationship between predicted and actual test lives.

Limitations and advantages of the Linear Strain Theory and the Smith Method of predicting fatigue life may now be listed.

LIMITATIONS

<u>Both Methods</u>

1. Need for S-N curves for smooth axially loaded specimens.

2. Need for stress-Strain curve for the material.

<u>Smith Method</u>

1. Need for a datum point representing the fatigue life of a structure wherein failure occurs at fewer cycles than the life represented by the nominal yield strength for the material when cycled at $R = 0$.

2. The structure supplying the datum point must have a stress concentration (not necessarily known). The method is inapplicable where no concentrations are present.

<u>Linear Strain</u>

1. Need for a stress concentration factor.

ADVANTAGES

Linear Strain Theory

1. Gives reliable predictions where stress concentrations are known

2. Does not require S-N data for the actual part.

Smith Method

1. Neither nominal stresses nor stress concentrations are needed, since stresses are found directly from the single test datum point. As presently conceived the single datum point represents the lifetime of a structure for constant level loading wherein failure occurs at a lifetime which is shorter than that represented by a smooth specimen cycled at its nominal yield strength at $R = 0$.

2. An extension of the method indicates that the datum point can be in terms of a known life for any given spectrum of loads, so long as the highest load in the spectrum caused yielding at the stress concentration where failure eventually occurred. This can be converted into lifetime for other load spectra or for correcting the original spectrum. The advantages of this would be self-evident in the form of time, money, and effort saved at the research, development, and production stages when a change in mission would otherwise necessitate another time-consuming program of destructive testing of a multimillion-dollar structure.

3. That the method is applicable to full scale structures is evident from the comparison of calculated to test lives of full scale structures tested by the Navy as shown in Figure 19.

SECTION VII

APPENDIX

TABLE I

Mechanical Properties of Materials Used in This Program

Material	Yield Strength (psi)			Ultimate Strength (Psi)			Elongation Per Cent
	High	Low	Average	High	Low	Average	Average
7075-T6	78,0000	73,000	76,000	86,000	81,000	83,000	12.0
2024-T3	51,000	57,000	54,000	75,000	72,000	74,000	21.0
2024-T81	63,000	66,000	65,000	68,000	71,000	69,000	11.0

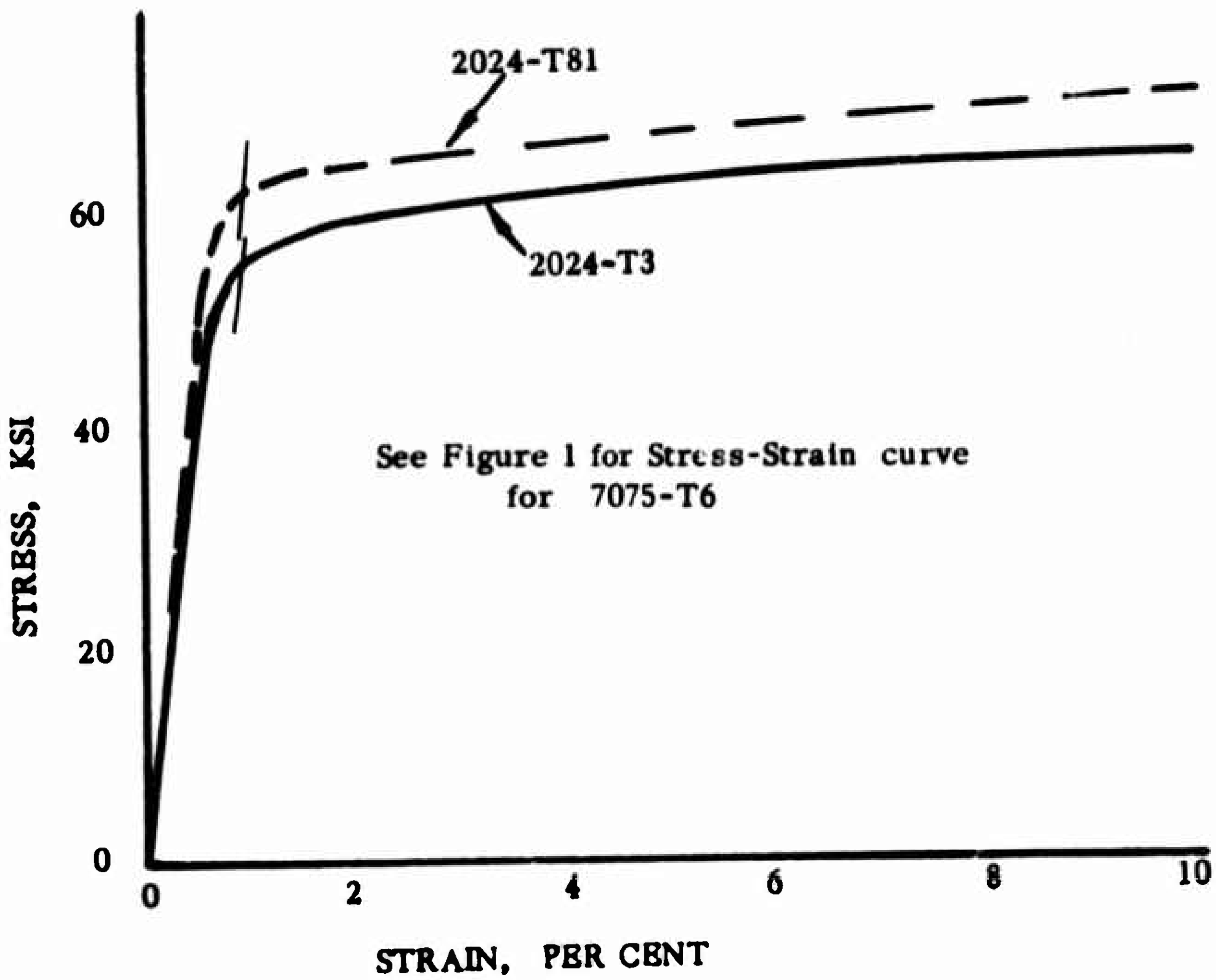

TABLE II

Constant Amplitude Fatigue Data for Smooth Axially Loaded Specimens of 0.1 Inch Thick 7075-T6 Aluminum Alloy

Stress Ratio	-4.0	-2.0	-1.0	-0.5	0	+0.25*	+0.5
Maximum Stress							
87,000					12		14
87,000					15		23
87,000					55		
87,000					1,663		
86,500					1,215		8
86,500					1,959		10
86,500					2,437		15
86,500					2,603		30
86,500					2,684		90
86,500					2,721		
86,500					3,154		
86,000				75	1,935		
86,000				95	2,105		
86,000				146	2,457		
86,000				859	2,651		
85,500							15
85,500							18
85,000				12	1,412		6,957
85,000				216	1,712		9,205
85,000					2,106		11,000
85,000					2,470		11,654
85,000					2,850		12,000
85,000					3,060		13,000
85,000							13,525
85,000							14,635

TABLE II, Contd

Constant Amplitude Fatigue Data for Smooth Axially Loaded Specimens of 0.1 Inch Thick 7075-T6 Aluminum Alloy

Stress Ratio	-4.0	-2.0	-1.0	-0.5	0	+0.25 *	+0.5
Maximum Stress							
84,000				410	3,235		
84,000				478	3,294		
84,000				640			
84,000				1,024			
83,000				850	1,795		
83,000				1,108	2,978		
83,000					3,198		
83,000					3,610		
83,000					190		
83,000					250		
82,000					1,095		
82,000					4,155		
81,000					3,030		
81,000					4,540		
80,000			85	1,195	2,225		
80,000			101	1,248	4,845		
80,000			135	1,370			
80,000			140	1,635			
78,000			55				
78,000			120				
78,000			196				
78,000			209				
77,500				1,266			
77,500				1,698			
77,000							11,000
77,000							21,000

TABLE II, Contd

Constant Amplitude Fatigue Data for Smooth Axially Loaded Specimens of 0.1 Inch Thick 7075-T6 Aluminum Alloy

Stress Ratio	-4.0	-2.0	-1.0	-0.5	0	+0.25*	+0.5
Maximum Stress							
77,000							25,000
77,000							25,000
77,000							26,000
75,000			285	2,649	6,000	10,000	
75,000			312	3,999	14,000	15,000	
75,000			360			16,000	
75,000			600			17,000	
75,000			883				
75,000			1,080				
72,000			298				33,000
72,000			302				49,000
72,000			320				50,000
72,000			530				
70,000			2,232		9,000		
70,000			3,300		11,000		
70,000					12,000		
70,000					14,000		
70,000					16,000		
65,000			2,043	7,000		17,000	83,000
65,000			2,160	8,000		21,000	92,000
65,000				9,000		21,000	103,000
65,000				10,000		27,000	
65,000				10,000			
60,000			2,940				51,000
60,000			3,600				75,000
60,000							99,000

TABLE II, Contd

Constant Amplitude Fatigue Data for Smooth Axially Loaded Specimens of 0.1 Inch Thick 7075-T6 Aluminum Alloy

Stress Ratio	-4.0	-2.0	-1.0	-0.5	0	+0.25*	+0.5
Maximum Stress							
60,000							336,000
60,000							2,015,000
55,000					28,000	38,000	252,000
55,000					36,000	45,000	735,000
55,000					39,000	57,000	2,820,000
55,000						78,000	6,865,000
53,000							53,000
53,000							64,000
53,000							87,000
53,000							294,000
50,000			11,000	18,000		58,000	
50,000			11,000	25,000		62,000	
50,000			13,000	25,000		87,000	
50,000			13,000	27,000			
50,000				27,000			
47,500						195,000	
47,500						221,000	
45,000					60,000	93,000	
45,000					81,000	237,000	
45,000					88,000	7,355,000	
45,000						8,522,000	
45,000						10,360,000	
40,000		940	21,000	35,000	51,000		
40,000		1,620	29,000	51,000	52,000		
40,000		2,985	35,000	52,000	100,000		

TABLE II, Contd

Constant Amplitude Fatigue Data for Smooth Axially Loaded Specimens of 0.1 Inch Thick 7075-T6 Aluminum Alloy

Stress Ratio	-4.0	-2.0	-1.0	-0.5	0	+0.25 *	+0.5
Maximum Stress							
40,000			40,000	72,000	130,000		
40,000				83,000	178,000		
35,000		2,565			84,000		
35,000		3,431			88,000		
35,000		4,526			201,000		
35,000		8,750			212,000		
35,000					678,000		
35,000					1,591,000		
35,000					2,230,000		
35,000					7,423,000		
32,500					167,000		
32,500					1,658,000		
32,500					4,616,000		
32,500					10,085,000→		
32,500					10,186,000→		
30,000		11,202	47,000				
30,000		22,702	95,000				
30,000		28,320	226,000				
30,000		28,493	235,000				
25,000		55,000	291,000	152,000	1,571,000		
25,000		71,000	645,000	209,000	4,455,000		
25,000		94,000	1,200,000	271,000	6,911,000		
25,000		111,000					
22,500	5,730			405,000			
22,500	8,978			1,200,000			
22,500	22,106			1,200,000			
22,500				1,362,000			

TABLE II, Contd

Constant Amplitude Fatigue Data for Smooth Axially Loaded Specimens of 0.1 Inch Thick 7075-T6 Aluminum Alloy

Stress Ratio	-4.0	-2.0	-1.0	-0.5	0	+0.25*	+0.5
Maximum Stress							
20,000	17,345	184,000	460,000				
20,000	19,200	272,000	629,000				
20,000		404,000	1,200,000				
20,000		412,000	1,200,000				
17,500		355,000					
17,500		378,000					
17,500		540,000					
17,500		569,000					
15,000	159,240	4,343,000					
15,000	162,000	5,251,000					
15,000	168,000	10,000,000 ←					
15,000	169,200	10,004,000 ←					
12,500	382,000						
12,500	628,000						

* Data for R = +0.25 and for stresses above 84,000 psi taken from Navy Contract No. N156-41307, "Development of a Method for Assessing the Effects of Cumulative Fatigue Damage of Metallic Structures". Report scheduled for publication in the Fall of 1964.

TABLE III

Constant Amplitude Fatigue Data for Smooth Axially Loaded Specimens of 0.1 Inch Thick 2024-T3 Aluminum Alloy

Stress Ratio	-2.0	-1.0	-0.5	0	+0.5
Maximum Stress					
74,000					15
74,000					18
74,000					21
73,500					13
73,500					15
73,500					20
73,250					18
73,000				23	15
73,000				24	65
73,000				42	24,259
73,000					24,756
72,000					40,205
71,500				4,760	
71,500				4,922	
70,000				5,851	
70,000				6,282	
70,000				6,515	
65,000			2,000	5,284	44,000
65,000			2,000	11,509	81,000
65,000			3,000		88,000
65,000					107,000
60,000				17,000	
60,000				19,000	
60,000				21,000	
60,000				23,000	
55,000					102,000
55,000					152,000
55,000					174,000
55,000					214,000
50,000		3,000	25,000	73,000	
50,000		5,000	26,000	96,000	
50,000		7,000	31,000	97,000	
50,000			32,000	120,000	
45,000					12,926,000

TABLE III, Contd

Constant Amplitude Fatigue Data for Smooth Axially Loaded Specimens of 0.1 Inch Thick 2024-T3 Aluminum Alloy

Stress Ratio	-2.0	-1.0	-0.5	0	+0.5
Maximum Stress					
40,000		15,000	80,000	98,000	
40,000		26,000	85,000	104,000	
40,000		31,000	110,000	184,000	
40,000		31,000	110,000	225,000	
40,000				327,000	
40,000				374,000	
35,000				259,000	10,000,000 →
35,000				561,000	
30,000		87,000	174,000	4,051,000 →	
30,000		99,000	238,000	16,570,000 →	
30,000		103,000	410,000		
30,000		119,000	591,000		
30,000		239,000			
27,500	11,000				
27,500	32,000				
27,500	40,000				
27,500	68,000				
25,000	68,000		147,000		
25,000	79,000		1,443,000		
25,000	82,000		4,282,000		
20,000	225,000	90,000	10,000,000 →		
20,000	229,000	422,000			
20,000	379,000	762,000			
19,000			10,000,000 →		
17,500	514,000				
16,000	1,476,000				
16,000	6,320,000				
15,000	10,000,000 →	10,232,000 →			
15,000	10,020,000 →	15,435,000 →			
15,000	10,118,000 →				

TABLE IV

Constant Amplitude Fatigue Data for Smooth Axially Loaded Specimens of 0.1 Inch Thick 2024-T81 Aluminum Alloy

Stress Ratio	-2	-1	0	+0.5
Maximum Stress				
80,000				2
77,000			5	6
77,000			6	7
77,000			10	8
75,000			33	13
75,000			45	13
75,000			52	75
75,000				3,000
72,500			34	
72,500			3,088	
72,500			3,960	
72,500			4,812	
70,000		21	4,743	31,000
70,000		24	5,683	42,000
70,000		31	6,565	49,000
70,000		61		
65,000				62,000
65,000				68,000
65,000				79,000
60,000		210	14,000	80,000
60,000		433	16,000	108,000
60,000		436	17,000	142,000
60,000		563		
55,000			30,000	
55,000			30,000	
55,000			36,000	
50,000		3,000	33,000	139,000
50,000		5,000	37,000	147,000
50,000		6,000	41,000	171,000
50,000				205,000
48,000				17,874,000
45,000			54,000	10,000,000
45,000			75,000	10,000,000
45,000			83,000	10,000,000
40,000		26,000	81,000	
40,000		28,000	209,000	

TABLE IV, Contd

Constant Amplitude Fatigue Data for Smooth Axially Loaded Specimens of 0.1 Inch Thick 2024-T81 Aluminum Alloy

Stress Ratio / Maximum Stress	-2	-1	0	+0.5
40,000		30,000	830,000	
35,000	1,056	44,000		
35,000	1,105	52,000		
35,000		68,000		
33,000			13,700,000	
30,000	2,000			
30,000	6,352			
30,000	13,999			
30,000	15,747			
27,500	11,000			
27,500	32,000			
27,500	40,000			
25,000	68,000	348,000		
25,000	79,000	420,000		
25,000	82,000			
20,000	225,000	5,056,000		
20,000	299,000	5,820,000		
20,000	379,000			
19,000		550,000		
19,000		10,000,000 →		
17,500	514,000			
16,000	1,476,000			
16,000	6,320,000			
15,000	10,000,000 →			
15,000	10,000,000 →			
15,000	10,000,000 →			

TABLE V

Constant Amplitude Fatigue Data for 7075-T6 Aluminum Alloy Lugs

Stress Ratio	-1		-0.5		0		+0.5	
Interference	0	0.003	0	0.003	0	0.003	0	0.003
Maximum Stress								
67,500						7	21	5
67,500						42	47	85
67,500						52	3,301	471
67,500							4,119	
65,000					500		30	63
65,000					635		35	2,298
65,000							120	2,755
65,000							138	4,100
65,000							450	
65,000							3,210	
65,000							3,459	
65,000							3,318	
65,000							3,512	
65,000							4,135	
60,000						574	4,338	2,945
60,000						625	4,719	3,064
60,000						698	5,520	3,248
60,000						759	6,017	4,161
50,000					1,278	1,170	7,000	5,000
50,000					1,320	1,230	7,000	7,000
50,000					1,511	1,440	8,000	7,000
50,000					1,546	1,591	8,000	8,000

TABLE V, Contd

Constant Amplitude Fatigue Data for 7075-T6 Aluminum Alloy Lugs

Stress Ratio	-1		-0.05		0		+0.5	
Interference	0	0.003	0	0.003	0	0.003	0	0.003
Maximum Stress								
45,000					1,732			
45,000					1,752			
45,000					1,807			
45,000					1,816			
45,000					2,006			
45,000					2,529			
42,000				3,000				
42,000				3,000				
40,000			4,000	10,000	2,735	6,000	12,000	11,000
40,000		4,000	4,000	15,000	3,520	7,000	13,000	13,000
40,000		4,000	6,000	21,000	3,680	7,000	14,000	22,000
40,000		6,000	7,000	26,000	4,373	9,000	15,000	24,000
40,000		7,000	8,000	30,000	5,000			
35,000		3,000	4,000	10,000		16,000		
35,000		5,000	6,000	12,000		16,000		
35,000		6,000	13,000	18,000		18,000		
35,000		13,000	15,000	19,000				
35,000		15,000		27,000				
30,000	7,000	42,000	8,000		9,000	37,000		
30,000	9,000	48,000	10,000		10,000	60,000		
30,000	10,000	49,000	11,000		10,000	72,000		
30,000	12,000				13,000	81,000		
25,000							23,000	63,000
25,000						107,000	39,000	69,000
25,000						108,000	41,000	135,000
25,000						152,000	58,000	248,000

TABLE V, Contd

Constant Amplitude Fatigue Data for 7075-T6 Aluminum Alloy Lugs

Stress Ratio	-1		-0.5		0		+0.5	
Interference	0	0.003	0	0.003	0	0.003	0	0.003
Maximum Stress								
22,500				185,000				60,000
22,500				196,000				90,000
22,500				201,000				229,000
22,500				273,000				
20,000	37,000	196,000	27,000		23,000			189,000
20,000	37,000	199,000	43,000		28,000			196,000
20,000	42,000	202,000	51,000		29,000			507,000
20,000	63,000	204,000			30,000			707,000
20,000								2,490,000
20,000								2,522,000
18,000								2,547,000
15,000		289,000	51,000	841,000	47,000	543,000		4,192,000
15,000		377,000	58,000	1,008,000	64,000	901,000		10,000,000
15,000		469,000	68,000	1,009,000	66,000	1,000,000		
15,000		618,000	91,000		534,000	1,086,000		
14,000							151,000	2,512,000
14,000							164,000	7,730,000
12,000		875,000					519,000	
12,000		922,000					1,022,000	
12,000		1,112,000						
12,000		1,257,000						
10,000			121,000	1,228,000	139,000		373,000	
10,000			135,000		183,000		388,000	
10,000			138,000		311,000		579,000	
10,000			253,000		404,000		814,000	
10,000					411,000			

TABLE V, Contd

Constant Amplitude Fatigue Data for 7075-T6 Aluminum Alloy Lugs

Stress Ratio	-1		-0.5		0		+0.5	
Interference	0	0.003	0	0.003	0	0.003	0	0.003
Maximum Stress								
8,000		1,403,000					1,449,000	
8,000							2,052,000	
8,000							2,680,000	
6,000	452,000	10,170,000					2,457,000	
6,000	506,000	12,856,000						
6,000	514,000							
6,000	687,000							
5,000	830,000		658,000		828,000			
5,000	1,471,000		744,000					
5,000	1,976,000		891,000					
5,000	1,978,000		1,117,000					
4,000					1,943,000			
4,000					2,189,000			
3,000					3,521,000			
3,000					3,697,000			
3,000					7,850,000			
2,500	1,841,000				6,725,000			
2,500	3,030,000				10,323,000→			
2,500	3,162,000							

TABLE VI

Constant Amplitude Fatigue Data for Lug Type Specimens of 2024-T3 Aluminum Alloy

Stress Ratio	-1.0		-0.5		0		+0.5	
Interference	0	0.003	0	0.003	0	0.003	0	0.003
Maximum Stress								
65,000					7			10
64,250								6
64,250								8
64,250								3,098
64,000								8
64,000								1,291
64,000								1,443
64,000								3,292
63,250						194		
63,250						226		
63,250						237		
63,000						20	8	118
63,000						25	8	1,113
63,000						215		2,045
63,000						279		2,078
63,000						286		3,335
62,750							51	
62,750							2,218	
62,750							2,641	
62,500					68		10	
62,500					303		987	
62,500					373		2,298	
62,500							3,908	
62,000					25	261		
62,000					191	293		

TABLE VI. Contd

Constant Amplitude Fatigue Data for Lug Type Specimens of 2024-T3 Aluminum Alloy

Stress Ratio	-1.0		-0.5		0		+0.5	
Interference	0	0.003	0	0.003	0	0.003	0	0.003
Maximum Stress								
62,000					341	293		
62,000					449			
60,000			9	9			4,304	
60,000			25	10			4,554	
60,000				220			5,208	
60,000				492				
57,000		10	410	428	690	557	5,049	3,614
57,000		20		440	738	721	5,925	4,202
57,000				543	765	735	6,129	5,188
57,000				871	895	842		5,601
55,000	13	195						
55,000	71	405						
55,000	198	414						
55,000	280	936						
55,000	409	1,260						
55,000	638							
54,000			492	303			7,000	
54,000			603	677			7,000	
54,000			820	692			8,000	
54,000			974	765			8,000	
53,000					1,020			
51,000			897					
51,000			990					
51,000			1,160					
51,000			1,298					

TABLE VI, Contd

Constant Amplitude Fatigue Data for Lug Type Specimens of 2024-T3 Aluminum Alloy

Stress Ratio	-1.0		-0.5		0		+0.5	
Interference	0	0.003	0	0.003	0	0.003	0	0.003
Maximum Stress								
50,000		642		928	919	1,000	8,000	8,000
50,000		858		1,000	1,384	1,000	9,000	9,000
50,000		951		1,117	1,488	1,000	11,000	10,000
50,000		1,158		1,310	1,660	1,245	13,000	11,000
50,000						1,334		
50,000						1,358		
50,000						1,629		
50,000						2,000		
47,000	1,082		1,349		1,821			
47,000	1,375		1,495					
47,000	1,602		1,522					
47,000			1,605					
45,000		1,359		1,718	2,128	1,283		
45,000		1,691		1,759		1,710		
45,000		1,769		1,955		1,772		
45,000		2,010		2,013		1,804		
44,000	1,680		1,669					
44,000	1,864		2,102					
44,000	1,961		2,323					
44,000	2,055		2,715					
43,000					2,429			
41,000	2,428		2,110		2,562			
41,000	2,545		2,161					
41,000	2,569		2,696					
41,000	2,989		2,751					

TABLE VI, Contd

Constant Amplitude Fatigue Data for Lug Type Specimens of 2024-T3 Aluminum Alloy

Stress Ratio	-1.0		-0.5		0		+0.5	
Interference	0	0.003	0	0.003	0	0.003	0	0.003
Maximum Stress								
40,000		1,960		2,703		2,000	18,000	17,000
40,000		2,598		3,261		5,000	21,000	22,000
40,000		3,118		3,370		5,000	22,000	24,000
40,000		3,553		3,991		5,000	32,000	33,000
39,000					2,722			
37,500					4,000			
37,500					5,000			
37,500					5,000			
37,500					6,000			
37,000					4,595			
35,000	3,816	3,939			4,996			
35,000	3,883	4,055			5,638			
35,000	4,548	4,360						
35,000	5,524	7,325						
32,500					7,983			
30,000	10,000	9,000	5,000	32,000	10,000	19,000	37,000	48,000
30,000	11,000	9,000	8,000	35,000	11,000	37,000	41,000	52,000
30,000	13,000	15,000	8,000	42,000	11,185	48,000	52,000	67,000
30,000	14,000	16,000	8,000	66,000	18,000	50,000	54,000	100,000
30,000					19,000			
25,000				83,000				
25,000				85,000				
25,000				91,000				
25,000				141,000				

TABLE VI, Contd

Constant Amplitude Fatigue Data for Lug Type Specimens of 2024-T3 Aluminum Alloy

Stress Ratio	-1.0		-0.5		0		+0.5	
Interference	0	0.003	0	0.003	0	0.003	0	0.003
Maximum Stress								
20,000	82,000	254,000	54,000	178,000	38,000	250,000	125,000	259,000
20,000	82,000	499,000	55,000	270,000	54,000	268,000	139,000	454,000
20,000	96,000	501,000	56,000	509,000	57,000	274,000	171,000	592,000
20,000	108,000	535,000	65,000	619,000	62,000	898,000	412,000	1,096,000
17,500								10,317,000 →
17,000								12,908,000 →
15,000	118,000	753,000		3,234,000				15,459,000 →
15,000	130,000	990,000		7,170,000				18,121,000 →
15,000	205,000	2,463,000						
15,000	298,000							
15,000	362,000							
14,500				773,000		5,067,000		
14,500				7,110,000		10,225,000 →		
14,500						10,284,000 →		
14,000				10,208,000 →		15,502,000 →		
14,000				12,645,000 →				
13,000						10,037,000 →	366,000	
13,000						10,278,000 →	421,000	
13,000							425,000	
13,000							465,000	
12,000						10,270,000	987,000	
12,000							1,157,000	
12,000							1,499,000	
11,750							458,000	
11,750							661,000	
11,500							513,000	

TABLE VI, Contd

Constant Amplitude Fatigue Data for Lug Type Specimens of 2024-T3 Aluminum Alloy

Stress Ratio	-1.0		-0.5		0		+0.5	
Interference	0	0.003	0	0.003	0	0.003	0	0.003
Maximum Stress								
11,000	492,000	2,239,000						
11,000	1,689,000							
10,500							803,000	
10,000	2,967,000	6,751,000	325,000		234,000	10,121,000		
10,000			431,000		253,000	16,020,000		
10,000			436,000		320,000			
10,000			457,000		530,000			
9,500		10,248,000					1,798,000	
9,500		12,736,000						
9,000	2,587,000						1,011,000	
8,500	5,373,000						1,579,000	
8,500	10,120,000						6,066,000	
8,500							3,220,000	
8,300	1,699,000							
8,250							10,242,000	
6,000					1,374,000			
5,500					1,402,000			
5,000			1,500,000		1,420,000			
5,000			2,287,000		10,000,000			
4,500			1,400,000		2,385,000			
4,500			1,608,000					
4,250					4,298,000			
4,250					9,255,000			
4,000			2,600,000		10,339,000			
3,750			1,856,000					
3,750			2,821,000					

TABLE VII

Constant Amplitude Fatigue Data for Center Hole Notched Specimens of 2024-T3, 2024-T81 and 7075-T6 Aluminum Alloy

Maximum Net Stress (PSI)	Cycles to Failure (R = 0)		
	2024-T3	2024-T81	7075-T6
53,000	1,706	3,458	3,015
53,000		5,262	3,178
53,000		5,574	5,330
53,000		6,008	
50,000		6,308	5,025
50,000			7,000
50,000			8,000
48,000	4,181		
48,000	4,514		
48,000	4,631		
48,000	4,718		
48,000	4,819		
45,000	5,078		9,000
45,000	6,488		10,000
45,000			15,000
45,000			17,000
40,000		12,650	28,000
40,000			30,000
40,000			31,000
40,000			36,000

TABLE VIII

Effect of Bolt Interference on Fatigue Life of 7075-T6 Aluminum Alloy Lugs (R = 0)

Maximum Stress (PSI)	0	0.001	0.002	0.003
40,000	2,735			4,000
40,000	3,520			5,000
40,000	3,680			7,000
40,000	4,000			7,000
40,000	4,373			7,000
40,000	5,000			10,000
30,000	7,000			42,000
30,000	7,000			56,000
30,000	8,000			56,000
30,000	9,000			63,000
30,000	9,000			67,000
30,000	9,000			70,000
30,000	9,000			73,000
30,000	9,000			85,000
30,000	10,000			
30,000	10,000			
30,000	13,000			
20,000	23,000		82,000	256,000
20,000	25,000		163,000	446,000
20,000	27,000		214,000	480,000
20,000	28,000		357,000	805,000
20,000	28,000			
20,000	29,000			
20,000	30,000			
20,000	34,000			
16,000			285,000	
16,000			289,000	
16,000			304,000	
16,000			321,000	
15,000	47,000			543,000
15,000	64,000			901,000
15,000	66,000			1,086,000
15,000				1,626,000
12,500		225,000		
12,500		236,000	3,355,000	
12,500		296,000	10,000,000	
12,500		543,000	10,000,000	

TABLE VIII, Contd

Effect of Bolt Interference on Fatigue Life of 7075-T6 Aluminum Alloy Lugs (R = 0)

Maximum Stress (PSI)	0	0.001	0.002	0.003
10,000	139,000			
10,000	183,000			
10,000	311,000			
10,000	411,000			
6,500				

TABLE IX

Effects of Prestressing on Subsequent Fatigue Life* of 7075-T6 Lugs (R = 0)

Prestress	0		30 KSI Prestress		35 KSI Prestress		40 KSI Prestress		50 KSI Prestress	
Interference	0	0.003	0	0.003	0	0.003	0	0.003	0	0.003
Maximum Stress (KSI)										
30							13	10	16	16
30							13	14	18	19
30							13	16	19	21
30							16	26	20	18
20	23	256	30	363	62	223	55	59	233	235
20	28	446	30	401	85	225	63	88	283	340
20	29	480	40	633	129	297	65	102	289	356
20	30	805	48	676		258	77	125	315	455
15	47	543	79	2,052	133		191	274		
15	64	901	83	3,008	157		114	321		
15	66	1,086	96		161		159	364		
15	58	1,000	138		210		213	406		
12.5	95									
10	404	2,547	590		426	2,150	2,476	1,841		
10	139	10,000	735		842	4,227	1,247	2,963		
10	183	2,490	865		1,961	6,535	1,608	3,125		
10	311		947		3,250		1,616			
10	411									

*Fatigue life presented in kilocycles to failure

TABLE X

Results of Spectrum Tests on Lug Specimens of 7075-T6 Aluminum Alloy

Sequences to Failure - See Figure 14

Test Condition	I		II				III	IV	V
Stress Ratio	0	-1.0	-0.5		0		0	0	0
Interference	0	0	0	0.003	0	0.003	0	0	0
	68	74	86	90	88	70	60	61	16
	83	78	88	92	94	76	72	65	87
	86	80	92	132	94	78	72	67	98
	87	92	94	138	96	80	75	68	98
	88	96	100	174	96	96	77	70	105
	96	100	104	194	98	122	80	71	107
	97	102	104	248	106	128	80	74	111
	102	104	108	272	106	134	89	81	119
	116	162	110		108	144		104	125
	134	214	120		110	146			129
		366				196			133
						256			140
Numerical Average	96	124	101	167	100	127	76	73	102
Median	92	100	102	166	97	123	76	70	109

TABLE XI

Results of Spectrum Tests on Lug Specimens of 2024-T3 Aluminum Alloy

Test Conditions	II	III			
Stress Ratio	0	-1.0	-0.5	0	
Interference	0	0	0	0	0.003
	102 126 144 146 148 176	113 131 174 203	135 147 157 163	130 153 164 186	195 338 440
Numerical Average	140	155	150	158	324

TABLE XII

Results of Spectrum Tests on Center Hole Specimens

Sequences to Failure - See Load Schedule

Test Condition	2024 - T3 I	2024 - T3 II	7075-T6 I	7075-T6 II	2024-T81 III
	156	236	184	234	199
	182	252	184	242	115
	198	264	190	294	120
	232	264	236	332	
	242	274			
Ave. Test	202	252	198	275	145
Lin. Strain	161	173	142	156	147
Smith	192	220	270	300	149

LOAD SCHEDULE

Maximum Stress	Minimum Stress	Cycles per Step per Sequence I	II	III
48,000	0	3		
40,800	0	17	17	
33,600	0	65	65	
26,400	0	172	172	
19,200	0	283	283	
19,610	5,032			630
23,162	5,032			202
26,162	0			90
30,303	5,032			32
33,855	-6,845			10
37,444	-12,728			4
40,996	5,032			1

TABLE XIII

Results of Spectrum Tests on Smooth Axially Loaded Specimens of 7075-T6 Aluminum Alloy

Test Condition (Fig. 14)	I			II			III			IV			V		
Stress Ratio	-1	-0.5	0	-1	-0.5	0	-1	-0.5	0	-1	-0.5	0	-1	-0.5	0
	6			9			9			5			20		
	7			15			10			5			24		
	11			17						7			29		
Ave. Test	8			13.7			9.5			5.7			24.3		
Calculated*	14.8			12.3			21.0			16.2			24.3		
		26			34			46			29			59	
		28			31			52			29			79	
		30			34			56			35			89	
					49			64			49			90	
Ave. Test		28.0			37.0			54.5			47.3			79.3	
Calculated*		42.2			38.5			55.0			42.5			54.0	
			78			85			188			136			208
			108			106			252			136			275
			136			106			200			154			275
			138			126			242			156			288
Ave. Test			115			105			220			145			261
Calculated*			109			107			150			152			196

* Using Miner rule. This is the only case where the Linear Strain and Smith Methods agree with Miner, there being no apparent residual stresses resulting from high loading. It should be noted that this does not apply to smooth bend specimens, since a residual stress will occur at the surface whenever the proportional limit is exceeded.

SECTION VIII

REFERENCES

1. Irwin, G. R., "Fracture Testing of High-Strength Sheet Materials Under Conditions Appropriate for Stress Analysis," U. S. Naval Research Laboratory (NRL Report 5486) Washington 25, D.C., July 27, 1960.

2. Hardrath, H. F., and McEvily, Arthur J., Jr., "Engineering Aspects of Fatigue Crack Propagation," Symposium on Crack Propagation, College of Aeronautics, Cranfield, England, September 26 through 28, 1961.

3. Paris, Paul C., Gomez, Mario P. and Anderson, William E., "A Rational Analytic Theory of Fatigue," from Trend in Engineering, Vol. 13, No. 1, University of Washington, January 1961.

4. Valluri, S. R., "A Unified Engineering Theory of High Stress Level Fatigue," Aeronautical Research Laboratory (ARL 181), Office of Aerospace Research, United States Air Force, Wright-Patterson Air Force Base, Ohio, December 1961.

5. Orowan, E., "Fundamentals of Brittle Behavior in Metals," Proceedings of the MIT Symposium, June 1950.

6. Griffith, A. A., "The Phenomena of Rupture and Flow in Solids," Phil. Trans. of the Royal Aero. Soc., London, No. 221, 1920.

7. Miner, M. A., "Cumulative Damage in Fatigue," J. of Applied Mechanics, Vol. 12, 1945.

8.

8. Palmgren, A., "Die Lebensdauer von Kugellagern," Zeitschrift Verdin Deutscher Ingenieure, Vol. 68, 1924.

9. Freudenthal, A. M., and Heller, R. A., "On Stress Interaction in Fatigue and a Cumulative Damage Rule," J. of the Aerospace Sciences, Vol. 26, No. 7, 1959.

10. Smith, C. R., "Influence of Residual Stresses and Stiffness Factors on Fatigue Strength of Metals and Structures," A lecture delivered at the Third Annual Engineering Symposium, Brigham Young University, Provo, Utah, April 21, 1962.

11. Corten, H. T. and Dolan, T. J., "Cumulative Fatigue Damage," International Conference on Fatigue of Metals, Inst. of Mech. Engrs. (London) and ASME (New York), September 1956.

12. Smith, C. R., "Prediction of Fatigue Failures in Aluminum Alloy Structures," Proceedings of the Soc. for Experimental Stress Analysis, Vol. XII, No. 2, 1955.

13. Gunn, K., "Effect of Yielding on the Fatigue Properties of Test Pieces Containing Stress Concentrations," The Aeronautical Quarterly, November 1955.

14. Ripp, F., Gomza, A., and Adee, T. C., "Calculation of Fatigue Life by Grumman Method and Comparison with Test Data," Grumman Aircraft Engineering Corporation Report No. GE-168, February 1959.

15. Smith, C. R., "Small Specimen Data for Predicting Life of Full-Scale Structures," Symposium on Fatigue Tests of Aircraft Structures: Low-Cycle, Full-Scale, and Helicopters, (ASTM Special Technical Publication 338). Presented at the Fourth Pacific Area Meeting of the American Society for Testing and Materials, Los Angeles, California, October 1 through 3, 1962. Published by ASTM, 1916 Race Street, Philadelphia, Pennsylvania, 1962.

16. Karry, R. W., and Dolan, T. J., "Influence of Grain Size on Fatigue Notch-Sensitivity," Technical Report No. 30, Research Project of Theoretical and Applied Mechanics, U. of Illinois, June 1952.

17. Peterson, R. E., Stress Concentration Design Factors, John Wiley & Sons, Inc., New York, 1953.